JOC The Journal of Organic Chemistry

pubs.acs.org/joc Article

Two Approaches for the Synthesis of Fused Dihydropyridines via a 1,6-Electrocyclic Reaction: Fluorescent Properties and Prospects for Application

Aleksey A. Gagarin, Polina O. Suntsova, Artem S. Minin, Varvara A. Pozdina, Pavel A. Slepukhin, Enrico Benassi,* and Nataliya P. Belskaya*

Cite This: https://dx.doi.org/10.1021/acs.joc.0c01934 Read Online

ACCESS | Metrics & More | Article Recommendations | Supporting Information

ABSTRACT: Reactions of penta-2,4-dienethioamides with acetylenedicarboxylic acid, methyl and ethyl esters, and methyl propiolate were systematically studied, and a number of new 2,3-dihydro-5*H*-thiazolo[3,2-*a*]pyridines (DTPs) and 4*H*,6*H*-pyrido[2,1-*b*][1,3]thiazines (PTZs) were prepared. A possible mechanism for a multistep domino transformation is suggested, and the key step is the 1,6-electrocyclic reaction. An additional alternative method for the synthesis of new heterocyclic systems was achieved. Evidence of the electrocyclic mechanism of a key step was collected from the analysis of the spatial structure of the synthesized bicyclic nonaromatic pyridines by X-ray diffraction and quantum chemical calculations, as well as from the thermodynamic quantities. DTPs exhibited yellow fluorescence in solution and yellow to red emissions in the solid state. Biological investigations demonstrated the ability of DTPs to penetrate living and fixed cells and presumably accumulate in lysosomes.

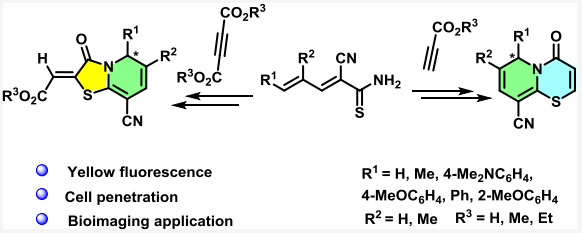

INTRODUCTION

Thioamides are building blocks widely used for the synthesis of nitrogen- and sulfur-containing heterocyclic compounds.[1−8] Thioamides can react with various monoelectrophilic, dielectrophilic, and ambient agents, such as α-halocarbonyl compounds and alkyl and alkenyl dihalides.[9−16] The C═S bond of a thioamide group may react as a dienophile component in [4 + 2] cycloaddition reactions[17−19] and as a dipolarophile in the thermal and catalytic variants of 1,3-dipolar cycloaddition reactions.[3,20,21] Moreover, α-diazothioacetamides easily transform into 1,2,3-thiadiazoles by a 1,5-electrocyclic reaction.[3,22−25]

A specific and significant group of thioamide transformations consists of reactions with acetylenedicarboxylic and propiolic acids and their esters.[5−8,26−34] These reactions are rather complicated due to the diversity of alternative directions caused by the multifunctionality of the reagents involved. Additional functionalities in the thioamide structure increase the number of active centers and expand their synthetic potential to obtain a variety of monoheterocyclic compounds, ensembles, and fused systems. Thus, thioamides bearing hydrazones, enamines, and multiple C═C lateral linear fragments have demonstrated new prospects for the construction of heterocycles with different ring sizes and various numbers and types of heteroatoms (Scheme 1).[5,29−31] These functionalities could affect the molecular electronic structure and thus could change the reaction direction or expand its scope. On the other hand, NH-hydrazone or enamine groups provide hydrogen atoms to facilitate heterocyclization (Scheme 1, reactions I and IIb).[29] Finally, the introduction of an additional C═C bond into a thioamide molecule forms the conjugative 1-thiabuta-1,3-diene fragment, which may be involved in the Diels−Alder reaction as a diene (Scheme 1, reactions IIa and III).[3,5,29−31] Moreover, the electronic effects of substituents, both proximate to and remote from the thioamide fragment, and the use of appropriate catalysts and solvents represent important factors for the control of the reaction progress (Scheme 1, reaction IIa and IIb). Sometimes these factors may make these reactions unpredictable, leading to unexpected products and requiring the verification of different conditions for their realization. Note that the most commonly used acetylenic derivatives are dimethyl acetylenedicarboxylate (DMAD) and methyl propiolate (MP), which are the most active in this series of reagents.

Herein, the results of our recent findings from ongoing research of these reactions are presented. The usage of new thioamide-bearing reagents (namely, penta-2,4-dienethioamide) in the interaction with acetylenic acids and their esters causes a series of subsequent transformations to afford new

Received: August 10, 2020

https://dx.doi.org/10.1021/acs.joc.0c01934
J. Org. Chem. XXXX, XXX, XXX−XXX

Scheme 1. Previous Examples of the Reactions of Thioamides Bearing Linear Lateral Functional Groups with DMAD and MP[29−31]

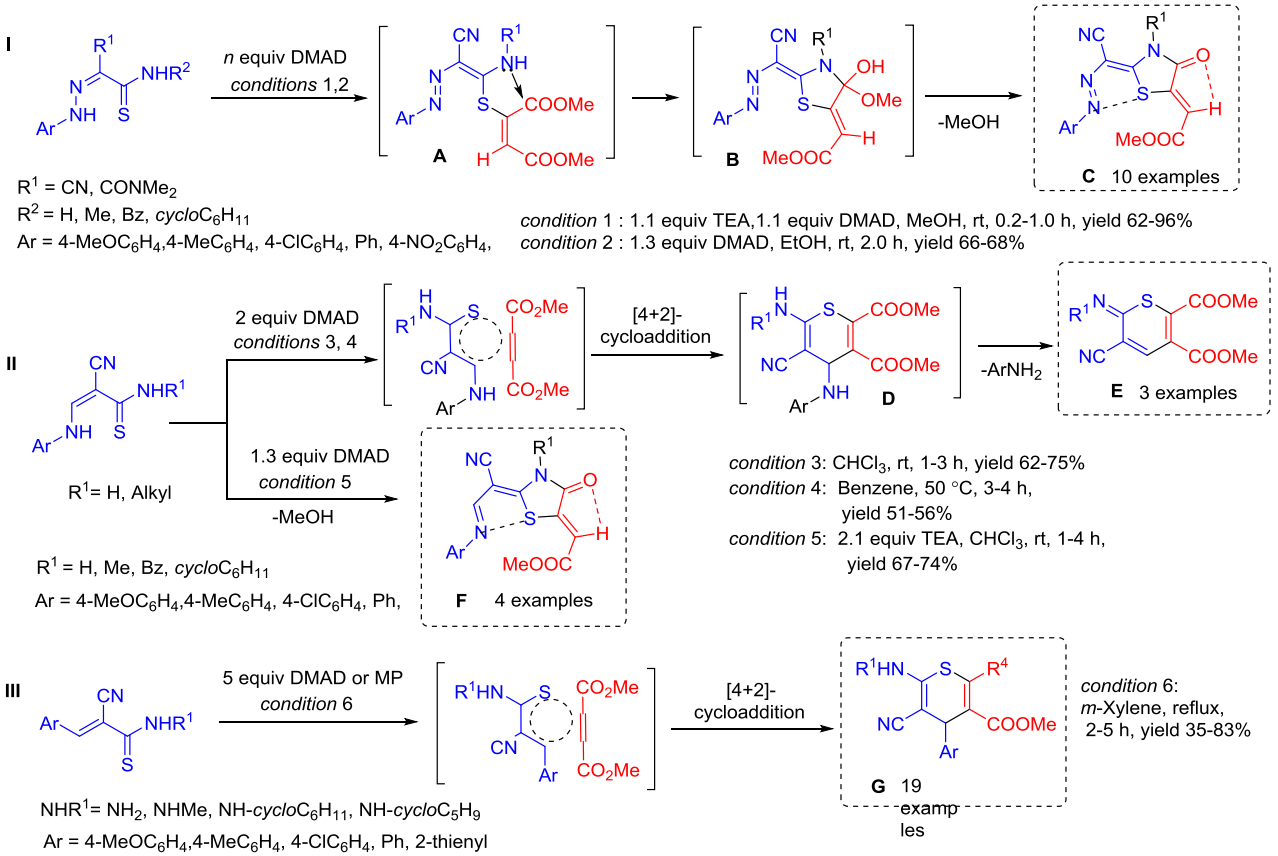

Table 1. Yields and Conversion Times for the Synthesis of 2-Cyano-5-phenylpenta-2,4-dienethioamide 3a by the Reaction of Aldehydes 1a and Cyanoethanethioamide 2[a]

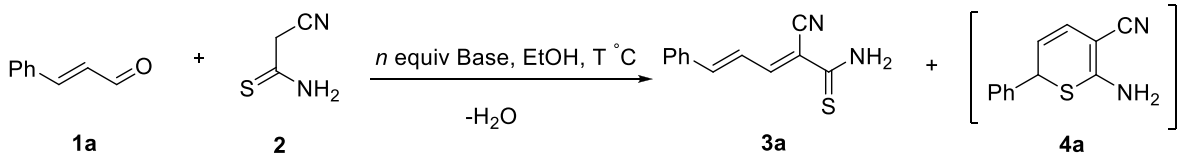

entry	*n* equiv	base[b]	*T* (°C)	time (h)	yield[c] (%)
1	0.05	NMM	rt	24.0	30
2	0.10	NMM	rt	5.0	65
3	0.05	TEA	rt	4.0	60
4	0.10	TEA	rt	3.0	65
5	0.05	TEA	40	4.0	71
6	0.10	TEA	40	6.0	50
7	0.05	TEA	60	2.0	46
8	0.05	TEA	60	3.0	48
9	0.10	TEA	60	0.5	95

[a]Reactions were performed 3−5 times, and the yield and conversion time used for the best experiments are presented. [b]Base: NMM, *N*-methylmorfoline; TEA, triethylamine. [c]Yield after separation and purification.

heterocyclic systems. Furthermore, the investigated reactions were performed by two synthetic procedures. On the one hand, one-pot conversion of thioamides and acetylene derivatives occurs through a series of sequential stages to yield bicyclic products. An alternative approach, which involves another sequence of stages, has important advantages as it prevents the formation of undesirable byproducts (thiopyrans), expands the scope of the reagents, and widens the library of new heterocycles.

RESULTS AND DISCUSSION

The synthesis of the starting reagents penta-2,4-dienethioamide **3a** and **3b** is described in the literature as the Knoevenagel condensation of cinnamaldehydes with cyanothioacetamide.[35−37] Unfortunately, the conditions suggested in these

https://dx.doi.org/10.1021/acs.joc.0c01934
J. Org. Chem. XXXX, XXX, XXX−XXX

Scheme 2. Condensation of Aldehydes 1b−e with Cyanothioacetamide 2

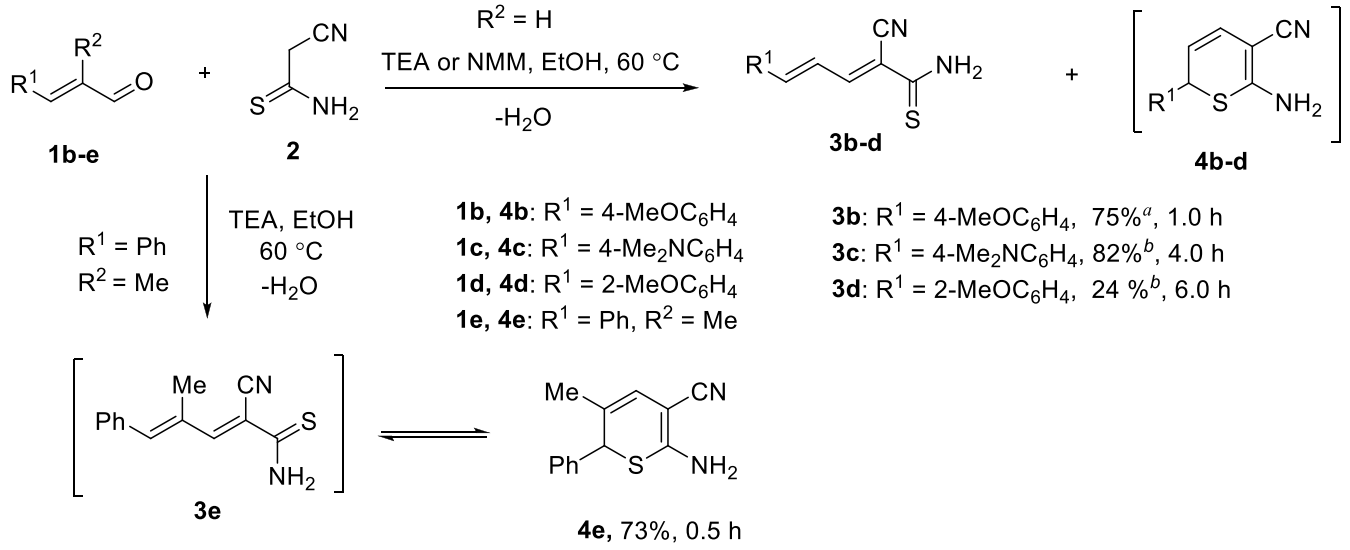

[a]With 0.1 equiv of TEA. [b]The best yield was obtained with 0.1 equiv of NMM.

Table 2. Multistep Domino Cyclization of 2-Cyanopenta-2,4-dienethioamide 3a with DMAD 5a

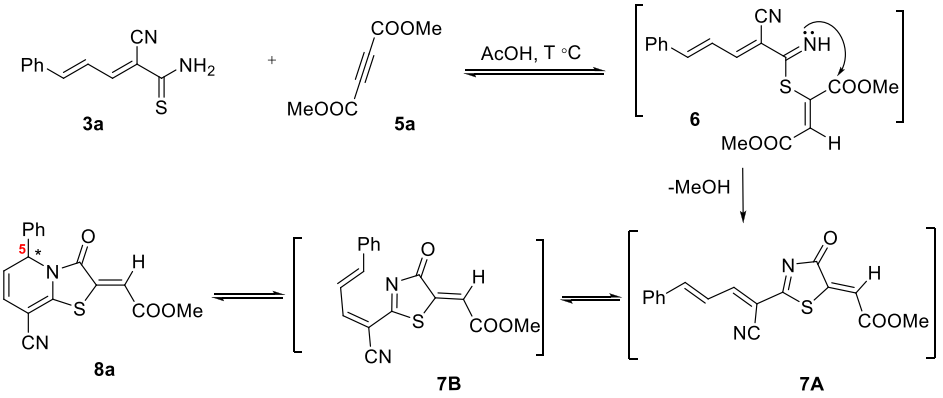

entry	solvent	T (°C)	time (h)	yield of **8a** (%)[a]
1	AcOH	rt	7.0	33
2	AcOH	60	1.0	40
3	AcOH	60	5.0	60
4	AcOH	60	7.0	78
5	AcOH	60	10.0	87
6	$CHCl_3$	rt	10.0	*b*
7	$CHCl_3$	60	10.0	*c*
8	MeOH	40	2.0	57

[a]Isolated yield. [b]Product not formed (TLC). [c]A mixture of compounds was formed (TLC).

publications did not reproduce the yield and transformation time described by the authors, which encouraged us to carry out a short study of the condition influence on the yield of penta-2,4-dienethioamide **3a** and the conversion time of starting reagents **1a** and **2** (Table 1). This reaction is very sensitive to the temperature, amount, and type of base used.

The heating of cinnamaldehyde **1a** with cyanothioacetamide **2** in ethanol at 60 °C in the presence of TEA gives penta-2,4-dienethioamide **3a** with an excellent yield at a fast rate. Although this condensation reaction also shows good results at room temperature, it takes a longer time to complete the transformation and leads to the formation and accumulation of byproduct. Subsequent experiments showed that this undesirable product presumably has a thiopyran structure, **4a**. It was identified (by thin-layer chromatography, TLC) at higher temperatures and required a careful procedure for purification.

This procedure was successfully used to obtain thioamides **3b**,**c**. In contrast, the yield of compound **3d** was below average (Scheme 2). Moreover, the condensation of α-methylcinnamic aldehyde (**1e**) with cyanothioacetamide (**2**) led to the formation of 2*H*-thiopyran-5-carbonitrile **4e** as the single product. This compound may be obtained as the result of the 1,6-electrocyclization of the initially formed 5-phenylpenta-2,4-dienethioamide **3e** (Scheme 2).

https://dx.doi.org/10.1021/acs.joc.0c01934
J. Org. Chem. XXXX, XXX, XXX−XXX

Table 3. Synthesis of 2,3-Dihydro-5*H*-thiazolo[3,2-*a*]pyridines 8b−j

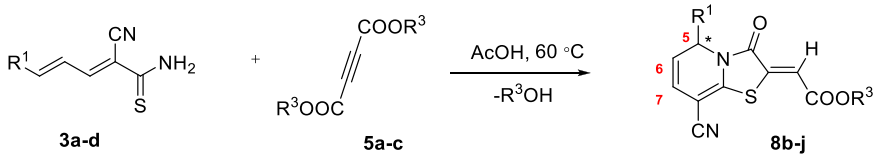

entry	compound	structure		time (h)	yield (%)[a]
		R^1	R^3		
1	**8b**	4-$MeOC_6H_4$	Me	1.0	66
2	**8c**	4-$Me_2NC_6H_4$	Me	1.0	50
3	**8d**	2-$MeOC_6H_4$	Me	1.0	38
4	**8e**	Ph	Et	5.0	45
5	**8f**	4-$MeOC_6H_4$	Et	10.0	78
6	**8g**	$Me_2NC_6H_4$	Et	5.0	30
7	**8h**	2-$MeOC_6H_4$	Et	48.0	48
8	**8i**	Ph	H	3.0	59
9	**8j**	4-$MeOC_6H_4$	H	1.0	68

[a]Yield after separation and purification.

Table 4. Synthesis of the 2,3-Dihydro-5*H*-thiazolo[3,2-*a*]pyridines along with the Second Procedure via the Initial Reaction of Aldehyde 1 by Condensation with Thiazolidinones 9a−c

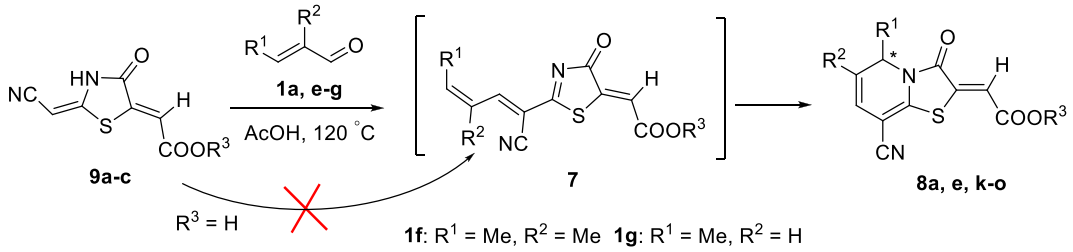

entry	compound	structure			time (h)	yield (%)[a]
		R^1	R^2	R^3		
1	**8a**	Ph	H	Me	15.0	39
2	**8k**	Ph	Me	Me	15.0	59
3	**8l**	Me	Me	Me	18.0	22
4	**8m**	Me	H	Me	14.0	15
5	**8e**	Ph	H	Et	14.0	34
6	**8n**	Ph	Me	Et	18.0	34
7	**8o**	Me	Me	Et	16.0	26

[a]Yield after separation and purification.

There are only a few known examples of thiopyran ring constructions by the 1,6-electrocyclization reaction, and this process usually requires very high temperatures.[38,39] Note that the cyclization of thioamide **3e** also proceeded at room temperature. Moreover, thiopyrans **4a−d** were identified by TLC during the reaction of aldehydes **1a−d**, with cyanothioacetamide **2** forming as a side product in a small amount. Because these reactions are accelerated by introducing subsequent electron-withdrawing and electron-donating substituents due to their resulting captodative effect,[40,41] the presence of an electron-donating substituent (Me) at the 5-position and CN group at the C(2) atom of the 1-thia-1,3,5-hexatriene system facilitates compound **1e** cyclization. This finding is very interesting for the theory of electrocyclic reactions and organic synthesis practices and certainly will be studied in further detail with the help of quantum mechanical calculations.

The structures of new compounds **3a−d** and **4** were characterized using spectroscopy, elemental analysis, and X-ray diffraction (XRD) data. The experimental procedures and spectral data of cinnamothioamides **3a−d** and thiopyran **4** are presented in the Supporting Information (Figures S1−S5).

The thioamide and acetylenic acid derivative interactions were studied in different solvents (AcOH, $CHCl_3$, MeOH, xylene, and benzene) and at different temperatures (from room temperature to a refluxing temperature).[4−6,26−34] We performed a series of preliminary experiments for the reaction of 2-cyano-5-phenylpenta-2,4-dienethioamide **3a** with DMAD **5a** in acetic acid, chloroform, and methanol, both at room temperature and by heating (Table 2).

The formation of a new compound occurred when the reagents were heated at 60 °C in acetic acid (TLC). The resulting product was isolated by column chromatography in a solvent system. Unexpectedly, the spectral data showed that the obtained compound **8a** was 2,3-dihydro-5*H*-thiazolo[3,2-*a*]-pyridine (DTP). We can therefore conclude that the reaction proceeds via the addition/condensation mechanism, which was

https://dx.doi.org/10.1021/acs.joc.0c01934
J. Org. Chem. XXXX, XXX, XXX−XXX

known previously (Scheme 1, I).[6,29,30] However, the investigated transformation did not stop at the cyclization stage and thiazolidinone **7** formation. As the active 1-aza-1,3,5-hexatriene system was created in intermediate compound **7**, the 1,6-electrocyclic reaction was initiated, and the pyridine ring fused to a thiazolidinone cycle and afforded the new heterocyclic dihydro-5*H*-thiazolo[3,2-*a*]pyridine system. Considering the known fact that such reactions facilitate systems simultaneously containing electron-donating and electron-withdrawing substituents, we can assume that acetic acid not only is a good solvent but also is capable of accelerating electrocyclization by enhancing the electron-withdrawing properties of triene system termini by protonating the nitrogen atom of the thiazole ring.

With this encouraging result, we continued our investigations to determine the scope of this reaction and all the synthesized thioamides, **3b−d**, and acetylenic acid and esters **5a−c** involved in the interaction (Table 3). All reactions afforded DTPs in a moderate or good yield (Table 4).

The best results in terms of yield were observed for the reaction of thioamide **3b** (Table 3, entries 1, 5, and 9). This finding agrees with the previously considered hypothesis that captodative substituents promote the 1,6-electrocyclic reaction. In addition, acetic acid may accelerate condensation with the acetylene reagents by activating their electrophilic centers and binding the eliminated methanol. The decrease in the yield of the reaction of thioamide **3c** with esters **5b**,**c** and the ineffectiveness of its interaction with acetylenic acid **5a** may be related to the partial protonation of this substituent nitrogen atom, which led to a decrease in its electron-donating properties.

The ^{1}H and ^{13}C NMR spectra, EI-TOF-MS spectra, and Fourier transform infrared (FT-IR) spectra were consistent with those of the structures expected for compounds **8** (see the Experimental Section and Figures S6−S15). Signals corresponding to the CH protons of the heterocyclic core were observed in the ^{1}H NMR spectrum of compound **8a** as a doublet of C(4)H doublets in the region of 6.02 ppm, whereas a doublet of C(5)H doublets of protons at 5.90 ppm and a doublet of doublets C(6)H at 6.23 ppm were observed with the corresponding constant. The correlation of the signals was based on 2D NMR experiments (Figure S6).

Clearly, the key compounds of this transformation are intermediates **7**, which may be obtained by condensation of the corresponding aldehydes with (5-ylidene-4-oxothiazolidin-2-ylidene)acetonitriles **9** (Scheme 3). The synthesis of

Scheme 3. Synthesis of (4-Oxothiazolidin-2-ylidene)acetonitriles 9a−c

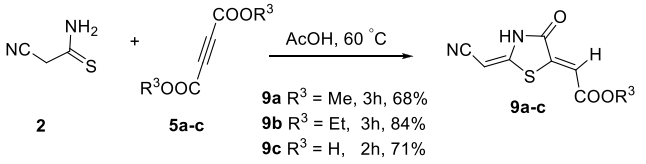

compounds **9a**,**b** from cyanoethanethioamide and esters **5a**,**b** (Scheme 4) is described in the literature.[31] Thus, with these compounds in hand, we could change the sequence of the transformation stages. Furthermore, with this type of reaction arrangement, we could avoid the side conversion of thioamides **3** into thiopyrans **4**, which was a fundamental obstacle for the effectivity and scope of this transformation.

Unlike the conditions proposed in the literature, we carried out this reaction by heating in acetic acid for electrophilic reagent activation. This change increased the yields of thiazolidinones **9a−c** and simplified the isolation and purification procedure (Scheme 3).

Furthermore, we carried out the condensation reaction of aldehydes **1a**,**e−g** with the obtained thiazolidinones **9a**,**b** in acetic acid. Indeed, this procedure led to the formation of new DTPs; however, it required a higher temperature (Table 4).

We also included crotonaldehyde and tiglic aldehyde in this interaction. However, the reaction was accompanied by the products of the degradation of the starting reagents. Nevertheless, DTPs **8l**,**m**,**o** were isolated using liquid column chromatography and identified by spectral methods (see Figures S20, S21, and 23). Our attempts to use 1,4-dioxane, ethanol, chloroform, and acetonitrile in combination with bases (NMM, TEA, AcONa, DIPEA, DBU) or acetic acid anhydride and conducting the reaction under refluxing conditions in a microwave reactor or in an argon atmosphere did not improve the yield. The reactions of aldehydes **1a−h** and acid **9c** were unsuccessful because acid **9c** was insoluble in acetic acid and some of the other organic solvents ($CHCl_3$, EtOH, MeCN, acetone, benzene).

To expand the scope of the starting reagent, we included the methyl ester of propiolic acid in this reaction (Scheme 4). The first synthetic procedure (I, Scheme 4), which started from the interaction of thioamide and methyl propiolate, allowed us to obtain only one new compound, **12a**. According to an alternative method (II, Scheme 4), we obtained thiazinone **10** and then used it in a reaction with other aldehydes. Indeed, this pathway allowed us to broaden the scope of 4*H*,6*H*-pyrido[2,1-*b*][1,3]thiazines (PTZs) **12b−e** by involving four additional aldehydes in the reaction.

Since their discovery, pericyclic reactions have attracted the attention of chemists due to the following unusual mechanism: new bonds are formed without the interaction of active intermediates but with the rearrangement of π-bond conjugative systems, thus leading to the construction of new σ-bonds and ring closures or to reverse processes.[42−48] This transformation proceeds in a stereoselective manner, forming well-organized transition states with a low activation barrier and very advantageous thermodynamic characteristics. Under thermal activation, 1,6-electrocyclization reactions were possible with hexatriene-conjugated systems of double bonds with 6π-electrons. During the formation of a new σ-bond, the terminal orbitals overlapped by disrotation, and depending on the direction of this motion, two diastereomers, **8A** and **8B**, might be formed (Scheme 5). Two rings of the heterocyclic core in the molecule of the product should be nonplanar. However, the presence of a nitrogen atom in the terminal position of the intermediate **7** heterohexatriene system could donate a pair of electrons to an orbital already located in the plane of the formed ring. This orbital could take part in new bond formation (a heteroelectrocyclic or pseudopericyclic mechanism).[3] In this case, only one orbital should turn, allowing overlap, and a new bond would form due to monorotatory cyclization. Thus, because of this reaction, enantiomers **8C** and **8D** should be formed, in which the DTP heterocyclic fragment was planar (Figure 1).

X-ray diffraction data obtained for a crystal of thiopyran **4a**, DTP **8a**, and PTZ **12a** that were grown from a dilute DMSO solution demonstrated that both rings of a heterocyclic core lie on the same plane, whereas the phenyl fragment deviates from

https://dx.doi.org/10.1021/acs.joc.0c01934
J. Org. Chem. XXXX, XXX, XXX−XXX

Scheme 4. Synthesis of PTZs 12a−e by Two Synthetic Approaches[a]

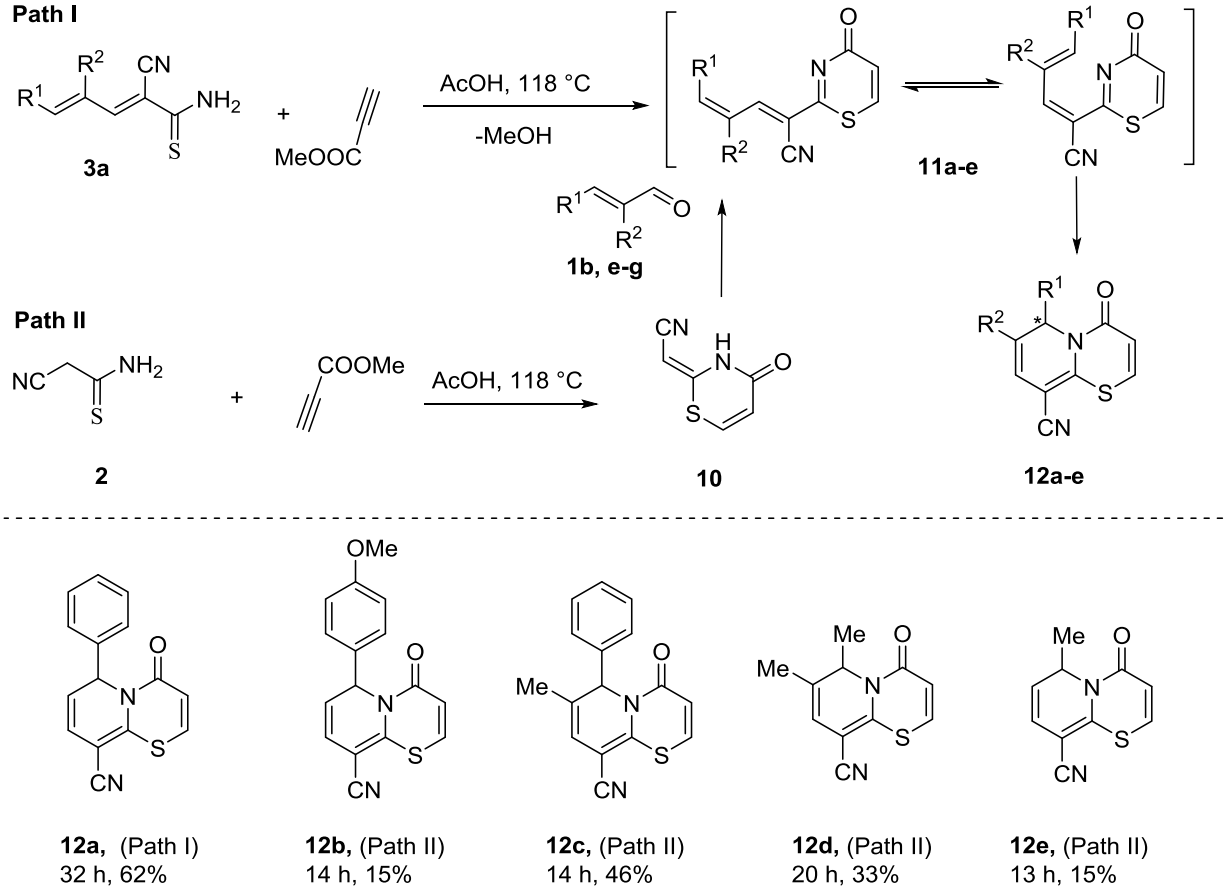

[a]Yield after separation and purification.

Scheme 5. Types of Terminal Orbital Rotations Occurring during the Cyclization of 1-Azahexatriene System Compound 7 to Form a DTP System

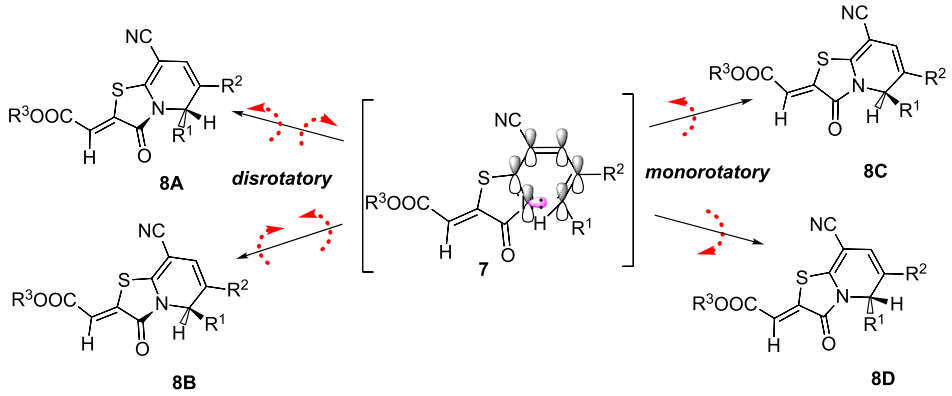

this plane by angles of 86.1 (for **8a**) and 89.9° (for **12a**) (Figure 1). Thus, the spatial arrangement of the cyclic fragments in thiopyran **4a**, DTP **8a**, and **12a** indicates a monorotatory variant of the electrocyclization of compounds **7** and **11** and the formation of *R*- and *S*-enantiomers, which are both present in the crystal.

The bicyclic flat structure of DTP **8a** was stabilized by a series of weak interactions between sulfur and oxygen atoms and between oxygen and hydrogen atoms, which held the lateral linear fragments in one plane (Figure 1) and, in fact, led to the formation of quasi-polycyclic molecules. This weak interaction nature was verified by the RDG plot (Figure 2),[49−52] which is a state-of-the-art technique based on electron density and is particularly reliable for investigating weak interactions.

RDG analysis clearly confirmed the existence of several van der Waals-type interactions (green-turquoise isosurface) and stronger bonding, in which sulfur binds with the oxygen atom (light-blue-colored isosurface) of the carbonyl group. These spatial features create the special architecture of the molecules, where most of the lateral fragments and substituents are held together by intramolecular electrostatic interactions.

To highlight the thermodynamics of the 1,6-electrocyclization stage compounds **3a**, **7a**, and **11a**, we performed quantum mechanical calculations at the density functional theory (DFT)

https://dx.doi.org/10.1021/acs.joc.0c01934
J. Org. Chem. XXXX, XXX, XXX−XXX

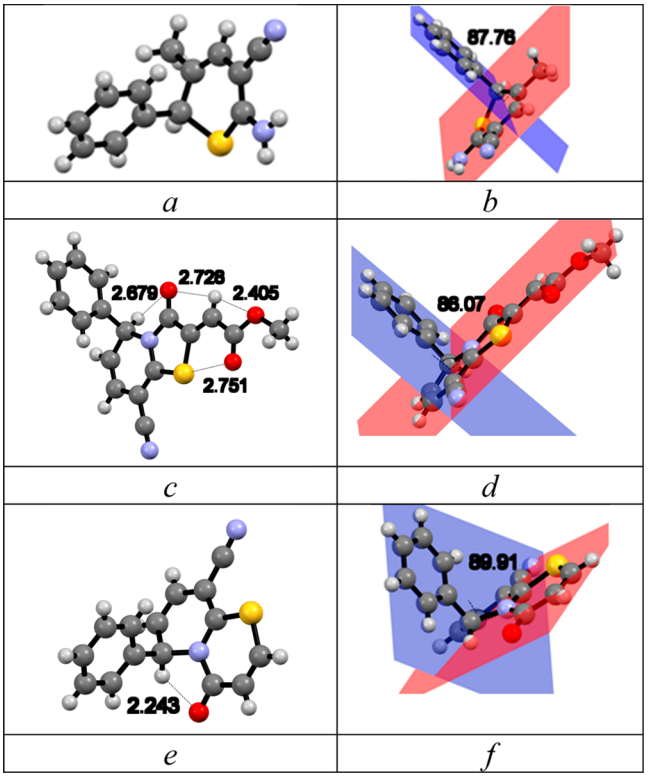

Figure 1. ORTEP view of thiopyran **4e** (a,b), DTPs **8a** (c,d), and PTZ **12a** (e,f) with thermal ellipsoids at the 50% probability level: (a,c,e) front view and (b,d,f) side view.

level, including examining solvent effects (AcOH) at 333 *K* (cf. Computational Details in the Supporting Information). The ΔG and ΔH values of the last stage of cyclization with the formation of thiopyran **4a**, DTP **8a**, and PTZ **12a** were calculated (Table 5 and Table S1) for the more stable rotamers.

A comparison of the thermodynamic quantities showed that the most favorable stage was cyclization to form DTP **8a**, in which the Gibbs free energy values were more negative than those of the other stages. ΔG_3 was also remarkably negative. Despite the cyclization to thiopyran being less probable, it was still possible. These findings agreed with the experimental data and the general rules of the 1,6-electrocyclization process.

Photophysical Properties of the DTPs. DTPs **8a**−**o** exhibited good solubility in DMSO, $CHCl_3$, CH_2Cl_2, and DMF, moderate solubility in EtOH, and poor solubility in hexane. Their solutions exhibited yellow emissions. The absorption and emission properties of the DTPs were studied in DMSO (Figure 3 and Table S2). The DTPs showed characteristic absorption bands at 301−325 and 419−437 nm in their electronic spectra and emission maxima at 552−559 nm. The unusually large Stokes shift (SS, up to 6487 cm^{-1}) was rationalized. The low intensity of emission may be caused by the remarkable loss of the absorbed energy via nonradiative processes during geometric relaxation due to the nonaromatic structure of the DTPs **8**.[53] DTP **8c** did not exhibit any fluorescence in the DMSO, DMSO−H_2O, or MeCN solutions. However, we observed the emission of this compound in DMSO after the addition of trifluoroacetic acid (TFA), which might be induced by the protonation of the $N(Me)_2$ substituent.

Further investigation of the DTP **8a** behavior in solvents with different properties showed that the dependence of the adsorption and emission parameters on the chosen solvent was negligible (Figure 4 and Table 6). Additionally, the quantum yield increased gradually, up to 2.72%, with decreasing solvent polarity.

Fluorophores used for biological research require their optical properties be characterized in water. As DTPs **8a**−**o** did not dissolve in water, we studied their optical properties in a 1:9 mixture of DMSO−H_2O (Table S2). The addition of water in this ratio did not cause the formation of suspensions or

Table 5. ΔG and ΔH Values of the 1,6-Electrocyclization Stage Leading to Thiopyran 4a, DTP 8a, and PTZ 12a

entry	1,6-electrocyclization stage	ΔG (kJ/mol)	ΔH (kJ/mol)
1	**3a** → **4a**	−11.7 to 8.5	−21.9 to 1.2
2	**7a** → **8a**	−67.9 to −50.8	−76.9 to −30.7
3	**11a** → **12a**	−49.3 to −35.7	−64.1 to −44.1

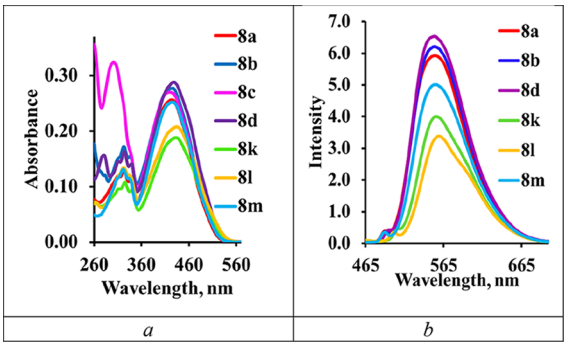

Figure 3. (a) Absorption and (b) fluorescence spectra of DTPs **8a-d** and **k-m** in DMSO. For the absorption measurements, $c = 2.5\times10^{-5}$ M, and for the fluorescence spectra, $c = 5\times10^{-6}$ M.

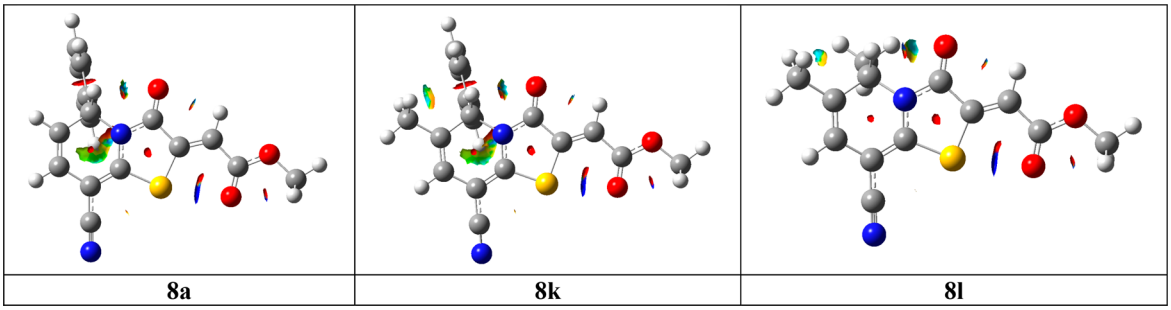

Figure 2. RDG plot of DTPs **8a**, **8k**, and **8l** in DMSO solution. NCI isosurface colors: red (strongly repulsive), yellow-green (weakly repulsive), green-turquoise (weakly attractive), and blue (strongly attractive). Atom color: white (H), gray (C), blue (N), red (O), and yellow (S).

https://dx.doi.org/10.1021/acs.joc.0c01934
J. Org. Chem. XXXX, XXX, XXX−XXX

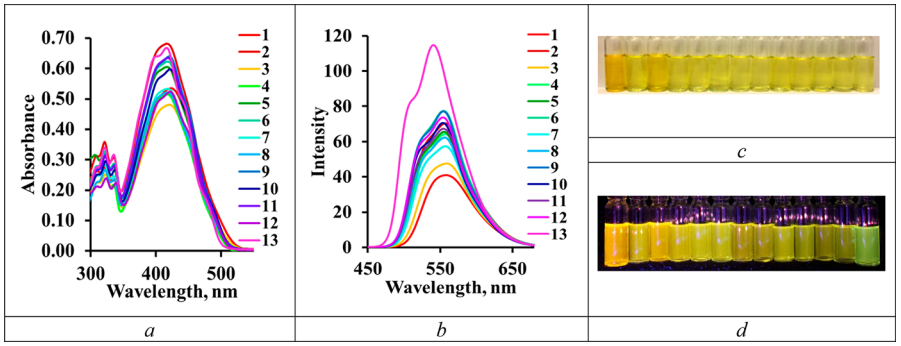

Figure 4. (a) Absorption and (b) fluorescence spectra of DTP **8a** in solvents with different polarities. For the absorption measurements, $c = 5 \times 10^{-5}$ M, and for the fluorescence spectra, $c = 5 \times 10^{-5}$ M. Photographs of the solutions of DTP **8a** exposed to daylight (c) and upon irradiation (d) with a hand-held UV lamp at 365 nm (solvents: 1, DMSO; 2, MeCN; 3, DMF; 4, acetone; 5, AcOEt; 6, AcO^{n}Bu; 7, EtOH; 8, THF; 9, CH_2Cl_2; 10, $CHCl_3$; 11, 1,4-dioxane; 12, toluene; 13, hexane).

Table 6. Photophysical Properties of DTP 8a in Different Solvents

entry	solvent	λ_{abs} (nm)[a,b]	ε (M^{-1} cm^{-1})	λ_{em} (nm)[c]	Stokes shift (nm/cm^{-1})	QY (%)[d]
1	DMSO	423	11400	559	136/5752	0.96
2	MeCN	420	11900	557	141/6085	1.46
3	DMF	421	10800	559	138/5864	1.19
4	acetone	416	10800	557	141/6085	1.64
5	AcOEt	416	11100	555	139/6020	1.80
6	AcOBu	418	11900	555	137/5905	1.75
7	EtOH	418	11900	558	140/6002	1.18
8	THF	418	11400	556	138/5938	1.51
9	CH_2Cl_2	420	12100	555	135/5792	1.92
10	$CHCl_3$	422	12200	553	131/5613	1.86
11	1,4-dioxane	418	11200	554	136/5872	1.90
12	toluene	422	11300	553	131/5614	2.20
13	hexane	416	12200	541	125/5554	2.72

[a]Absorption measured in a solution with a concentration of 5×10^{-5} M. [b]Only the longest absorption maxima are reported. [c]Emission measured at a concentration of 5×10^{-5} M. [d]Quantum yield (QY) is measured relative to quinine sulfate (λ_{exc} = 366 nm; Φ = 0.53).

aggregates; moreover, deviations in the shape of the spectra are not observed. In general, the maximum absorption and emission showed a slight red shift. The QY decreased by ~1.2−5.5-fold, and a larger QY decrease was observed for **8b** and **8f** due to the MeO substituent located at the C(5) aromatic ring.

The solid DTP samples exhibited dark yellow to brick red colors and yellow and red emissions upon irradiation (Figure 5 and Table 7). Emissions from the solid samples were observed between 556 and 598 nm. Thus, the potential of the novel heterocyclic core in the solid-state emission (SEE) family and multifunctional fluorophore was demonstrated.[54]

The mechanism of solid-state fluorescence is usually explained by the restriction of intramolecular rotation (RIR) due to twisted propeller-like molecular conformations and decreasing nonradiative energy loss.[53] Thus, we can suggest that, for investigated DTPs **8**, solid-state emission may occur owing to the specific spatial location of the aromatic cycle at the C(5) atom of the heterocyclic score (Figure 1c,d).

To conclude, the newly synthesized heterocyclic compounds exhibited absorption in the visible range of the spectra and weak but yellow fluorescence, despite their short-conjugated system. Moreover, the C(5) aromatic ring was located perpendicular to the plane of the central heterocycle (XRD data, Figure 1c,d).

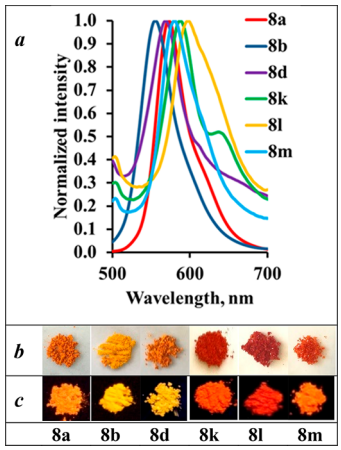

Figure 5. (a) Emission spectra of DTPs **8a−d,k−m** in the solid state. Photographs of DTPs **8a−d,k−m** under irradiation with (b) sunlight and (c) hand-held UV lamp at an emission wavelength of 380 nm.

Table 7. Absorption and Emission Values of DTPs 8a,b,d,k−m in the Solid State

entry	compound	λ_{exc} (nm)	λ_{em} (nm)	QY (%)	SS (nm/cm^{-1})
1	**8a**	463	573	1.58	110/4146
2	**8b**	417	556	0.88	139/5995
3	**8d**	463	570	1.21	107/4054
4	**8k**	463	587	1.02	124/4562
5	**8l**	463	598	0.64	135/4876
6	**8m**	463	580	0.80	117/4357

Such absorption and emission characteristics may be explained by the presence of numerous heteroatoms with additional lone pairs, the planarity of the heterocycle, and the lateral C═C double bond.

Quantum Mechanical Calculations. To study the DTP behavior upon excitation and emission, we analyzed the geometry and electronic structure at the ground state (GS) and excited state (ES), including the effect of solvation (DMSO and MeCN). (All details of the quantum mechanical calculations are presented in the Supporting Information.) The possible rotamers of **8a,k,l** were investigated, and the most stable rotamers were established and used for the subsequent calculations. The geometry of the most stable rotamers in the ground and excited states are presented in the Supporting Information (Figure S33 and Tables S3−S6). The main

https://dx.doi.org/10.1021/acs.joc.0c01934
J. Org. Chem. XXXX, XXX, XXX−XXX

Table 8. Computed Absorption Wavelength (λ_a), Oscillator Strength (f_{01}), Emission Wavelength (λ_e), Oscillator Strength (f_{10}), Modulus of Electric Dipole Moments in the Ground State (μ_0), Vertical Franck−Condon Excited State (μ_{1v}), Relaxed Excited State (μ_{1r}), and Angles Formed by the Dipole Moment Vectors ($\theta_{0,1v}$ and $\theta_{0,1r}$) for the Most Stable Rotamer of DTPs 8a, 8k, and 8o in DMSO and MeCN

entry	compound (solvent)	λ_{01} (nm)	f_{01}	μ_0 (D)	c_{H-L}	λ_{em} (nm)	f_{10}	c_{L-H}	μ_{1v} (D)	μ_{1r} (D)	$\theta_{0,1v}$ (deg)	$\theta_{0,1r}$ (deg)
1	**8a** (DMSO)	423	0.6828	6.0	0.68485	562	0.6012	0.69288	6.4	7.3	88.2	92.8
2	**8a** (MeCN)	417	0.6802	5.9	0.68490	560	0.5980	0.69292	6.4	7.3	88.1	92.6
3	**8k** (DMSO)	429	0.6971	6.3	0.68610	558	0.6210	0.69483	7.9	8.9	90.1	94.1
4	**8k** (MeCN)	427	0.6944	6.3	0.68620	558	0.6180	0.69487	7.9	8.8	90.0	93.9
5	**8o** (DMSO)	436	0.7081	6.3	0.68693	561	0.6257	0.69573	8.2	9.2	109.5	112.3
6	**8o** (MeCN)	427	0.7055	6.3	0.68701	557	0.6231	0.69577	8.2	9.1	109.2	111.9

structural peculiarities of compounds **8a,k,l** are the planarity of the heterocycle core and double C═C bond. The aromatic ring and central heterocycle are almost perpendicular to each other. The geometry of DTPs **8a,k,o** changes insignificantly upon excitation. The bond lengths in their molecules, as well as the S···O noncovalent interaction, tend to decrease (by ∼1%), whereas the intramolecular O···H hydrogen bond becomes weaker.

Furthermore, we analyzed the electronic features of the ground and excited state DTPs **8a,k,l** (Table 8). The electric dipole moment increases insignificantly upon excitation and emission, whereas the direction changes from 88.1 to 112.3°. The wavelength values calculated for the absorption and emission maxima, both in DMSO and in MeCN, were close to the experimental ones, which confirms the applicability of the method used and its potential for investigating the electronic structure of the studied compounds. The electronic transitions are essentially HOMO−LUMO excitations.

For these molecules, HOMOs were delocalized on the bicyclic core and C═C bond, whereas LUMOs were slightly shifted to ethoxycarbonyl fragments (Figure 6), suggesting

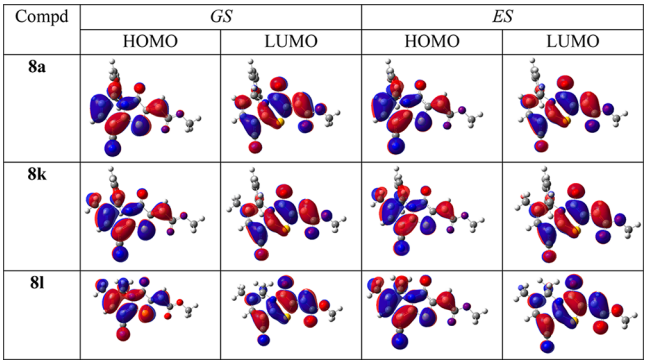

Figure 6. Frontier molecular orbitals, HOMO and LUMO, in the ground (left) and excited states (right) for DTPs **8a,k,l** in DMSO (|isovalue(MO)| = 0.02 au; |isovalue(ρ)| = 0.0004 au).

negligible intramolecular charge transfer[53,55−57] from the donor to the acceptor moieties upon photoexcitation and emission. The HOMO and LUMO exhibited remarkable overlapping of the interacting orbitals upon excitation and emission. This was supported by the large oscillator strengths for both absorption and emission. The phenyl ring is not involved in the HOMO or LUMO in either the ground or excited states due to its spatial location.

The map of the molecular electrostatic potential (MEP)[58,59] confirms that DTPs have many sites for nucleophilic and electrophilic attack, the formation of hydrogen bonds, and other weak interactions (Figure 7). The negative electrostatic

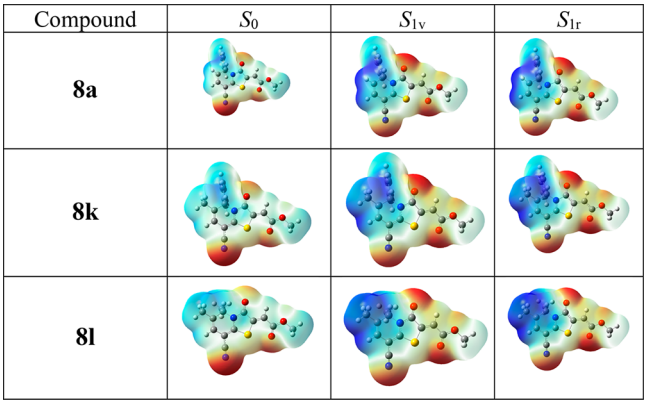

Figure 7. Plot of the MEPs of ATAs **8a**, **8k**, and **8l**, as calculated by time-dependent DFT at the ω-B97X-D/6-311++G**//IEF-PCM (UFF) level of theory, for the ground and excited states in DMSO. Map colors: red (negative potential), blue (positive potential). Elements: hydrogen (white), carbon (gray), nitrogen (blue), oxygen (red), sulfur (yellow) (range, −0.05 to 0.05 au; density |isovalue| = 0.0004 au).

potential of the DTPs was associated with the presence of the oxygen atoms and nitrogen of the CN group, and the positive potential was related to the hydrogens of the pyridine ring. All centers became more active upon excitation.

Bioassay Studies in Living and Fixed Cells. The design and preparation of new fluorophores to exploit their applications in life science provides new opportunities for biology and biomedical research. For biomedical applications, fluorophores that can visualize the evolution of biological processes and image interactions between fluorophores and biomolecules are highly desired. To determine the prospects of DTPs for their use in biology and medicine, we investigated the ability of these produced substances to stain cells for fluorescence microscopy.[60−63] Compounds **8a−o** exhibited maximum absorption in the visible region. This was an advantage for their use in biological experiments as exposure to visible radiation is safer for living organisms and living cells than exposure to UV radiation.

A green monkey epithelial cell culture (Vero) was used for the biological experiments. After being stained and washed, preparations of living cells were examined using an LSM-710 confocal laser scanning microscope (CLSM, Carl Zeiss) with a multichannel QUASAR detector (34 channels). Lasers at wavelengths of 405 and 488 nm were used. Images were obtained using an immersion lens (40×, 1.3 oil) with a resolution of 1024 × 1024 pixels and an image size of 212 × 212 μm. To obtain an informative fluorescent image using special software ZEN (Carl Zeiss), a special lambda mode (λ-

https://dx.doi.org/10.1021/acs.joc.0c01934
J. Org. Chem. XXXX, XXX, XXX−XXX

mode) was used, which allowed for the determination of the emission range with the maximum contrast for this preparation.

The above-mentioned study showed that the **8a** and **8k** substances penetrated into the cell and accumulated as separate bright points, most likely in lysosomes (Figure 8). The

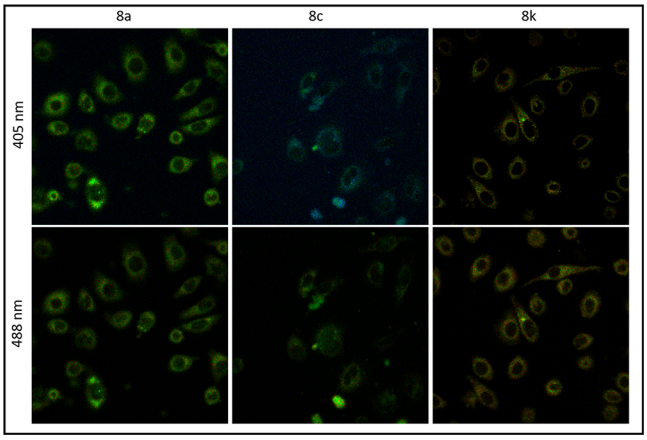

Figure 8. CLSM images of Vero cells incubated with DTPs **8a**, **8c**, and **8k** (1.0 μM) in DMEM for 0.5 h at 37 °C. The CLSM images were obtained with 405 and 488 nm excitations, and a 488−600 nm long-pass collection filter was used to generate the overlaid images.

fluorescence intensity of **8c** was somewhat lower than that of the other compounds; therefore, no definite conclusion on its accumulation could be drawn. None of the test substances penetrated the cell nucleus. Substances **8a** and **8k** fluoresced in the yellow range (550−580 nm) when excited by both lasers with wavelengths of 405 and 488 nm.

A very similar pattern was observed in cells stained with **8a**, except that the fluorescence response was slightly shifted to the blue region (510−550 nm). The fluorescence intensity of the **8a** substance was less than that the other substances in the cells, and the fluorescence spectrum of **8a** differed when it was excited by a laser with a wavelength of 405 nm, showing a fluorescence shift in the blue region (450−500 nm). When excited at 488 nm, the fluorescence response was yellow-green (500−550 nm). Importantly, the DTPs did not cause any visible toxic effect on the cells and cellular organs.

In fixed cells, the results were significantly different. The fluorescence intensity of the dyes significantly decreased. Substances **8a** and **8c** in fixed cells fluoresced so dimly that it was impossible to obtain a high-quality image. All of the substances stained the cells, whereas the accumulation of dye in the nucleus was observed; thus, the nucleolus was clearly distinguished. The fluorescence spectrum of all three substances was in the blue-green region. Note that DTP **8c** was nonfluorescent in DMSO and DMSO−H_2O (1/9), and only the addition of TFA to the DMSO solution led to an emission (Table S1, entries 8 and 10). Thus, the interaction of DTP **8c** with biological objects induced appreciable fluorescence.

Conclusions and Outlook. The synthesis of 1-aryl-2-cyanopenta-2,4-dienethioamides was carried out, and their reaction with acetylenedicarboxylic acid, ester derivatives, and methyl propiolate was rationalized. The reaction pathway led to the formation of an active intermediate bearing a 1-azahexatriene chain, which was involved in the 1,6-electrocyclic reaction to construct two new heterocyclic systems, namely, 2,3-dihydro-5*H*-thiazolo[3,2-*a*]pyridines and 4-oxo-4*H*,6*H*-pyrido-[2,1-*b*][1,3]thiazines. The results obtained according to an alternative procedure with another step sequence, along with the specific three-dimensional structure studied by XRD data, quantum mechanical calculations, and the thermodynamic characteristics of the 1,6-electrocyclic reaction, supported the transformation mechanism.

However, studying and proving the detailed and accurate mechanism of a chemical reaction is a rather complex task and requires dedicated experimental and theoretic investigations, including a variety of different methods and approaches, which are currently underway. These results will allow us not only to define the geometry and thermodynamics of the transition state but also to prove the correct classification of the new example of the 1,6-electrocyclic reactions and their place in pericyclic transformations. Furthermore, we hope to establish the specificity of the reactivity of the active intermediates and relationships between their structure and reactivity and to expand the scope of the reagents and variation in the new heterocyclic products for specific applications.

Despite the scarcity of π-electrons in their structure and the high nonaromaticity of the obtained 2,3-dihydro-5*H*-thiazolo-[3,2-*a*]pyridines absorbed in the visible region, they demonstrated yellow emissions.

Biological assays showed that DTPs penetrated through the cellular membrane and presumably accumulated in lysosomes without any undesirable effects on the cells and cellular organelles. Therefore, DTPs could also realize fluorescence visualization in living systems, thereby providing live cell imaging for the transport of biologically active compounds or natural compounds and diagnostic molecules to biotargets. The pathways in this study have real application prospects due to the numerous functional groups in molecular DTPs. In-depth studies on the fluorescence properties of new DTP derivatives and further applications of the synthesized fluorophores are currently ongoing.

EXPERIMENTAL SECTION

Materials and Methods. ^{1}H NMR and ^{13}C NMR spectra were recorded with a Bruker Avance II (Karlsruhe, Germany) (400 MHz for ^{1}H, 100 MHz for ^{13}C) spectrometer. Chemical shifts are reported in parts per million (ppm) relative to TMS in ^{1}H NMR and to the residual solvent signals in ^{13}C as an external reference. Coupling constant (*J*) values are given in hertz (Hz). Signal splitting patterns are described as a singlet (s), doublet (d), triplet (t), quartet (q), sextet (sext), quintet (quin), multiplet (m), broad (br), doublet of doublets (dd), doublet of triplets (dt) or AA′XX′, spin system of para-substituted benzene with two different substituents. The major isomer signal is highlighted with an asterisk (*). The ^{13}C NMR signal patterns for several compounds were determined by APT (attached proton test) and are described as follows: "+" for secondary or quaternary carbon atoms (positive signal) and "−" for primary or tertiary carbon atoms (negative signal). Mass spectra were recorded with a Shimadzu GCMS-QP 2010 "Ultra" (Kyoto, Japan) mass spectrometer using the electron impact (EI) ionization technique (70 eV). The abbreviation $[M]^+$ refers to the molecular ion. High-resolution mass spectra were obtained using an Agilent 6545-Q-TOF (Agilent Technologies Inc., Santa Clara, CA, USA) mass spectrometer equipped with an ESI source operating in positive ionization mode with a resolution of 15000 (fwhm). The FT-IR spectra were obtained using a Bruker Alpha (NPVO, ZnSe) spectrometer (Ettlingen, Germany). Elemental analyses were carried out using a PerkinElmer 2400 Series II CHNS/O analyzer (Shelton, CT, USA). Melting points were determined with a Stuart SMP3 apparatus (Staffordshire, ST15 OSA, UK).

UV−vis absorption spectra were recorded with a PerkinElmer Lambda 35 UV−vis spectrophotometer (Shelton, CT, USA). Fluorescence of the sample solutions was measured using a Hitachi F-7000 spectrophotometer (Tokyo, Japan). The absorption and

https://dx.doi.org/10.1021/acs.joc.0c01934
J. Org. Chem. XXXX, XXX, XXX−XXX

emission spectra were recorded in hexane, toluene, 1,4-dioxane, $CHCl_3$, CH_2Cl_2, EtOH, AcO^{n}Bu, AcOEt, DMF, MeCN, and DMSO using 10.00 mm quartz cells. The excitation wavelength was determined at the absorption maxima. Atmospheric oxygen contained in solutions was not removed. The concentrations of the compounds in the solution were 2.5×10^{-5} and 5.0×10^{-5} M for absorption measurements and 5.0×10^{-5} and 5.0×10^{-6} M for fluorescence measurements. The relative fluorescence quantum yields (Φ_F) were determined using quinine sulfate in 0.1 M H_2SO_4 as a standard (Φ_F = 0.546). The absolute quantum yield for the solid-state and time-resolution study was recorded with a Horiba FluoroMax 4 spectrofluorometer (Kyoto, Japan) with a Quanta-φ integrating sphere using FluorEssence 3.5 software.

The reactions were monitored by analytical TLC on aluminum-backed silica gel plates (Sorbfil UV-254). Visualization of components was accomplished by short wavelength UV light (254 nm). Solvents were dried and distilled according to common procedures. All solvents were of spectroscopic grade. Aldehydes **1a**−**e** and acetylenes **5a**−**e** were obtained from Acros Organics and used without further purification. Cyanthioacetamide **2** is known compound and was obtained by the literature procedure.[62]

Preparation and Characterization of Compounds. *General Procedure A (GP-A): Synthesis of the Penta-2,4-dienethioamides **3a**−**3d** and Thiopyrane **4**.* TEA (1.0 mmol, 0.140 mL) was added to a flask containing a solution of cyanothioacetamide **2** (10.0 mmol, 1.000 g) and aldehyde **1** (10.0 mmol) in EtOH (5.0 mL). The reaction mixture was stirred at 60 °C under oil-bath heating for 0.5−6.0 h until the TLC analysis indicated total consumption of the starting cyanothioacetamide **2**. The resulting mixture was cooled in an ice bath for 0.5 h. The precipitate was collected by filtration, washed with small quantities of ethanol, and dried.

*General Procedure B (GP-B): Synthesis of the DTPs **8a**−**j**.* To a solution of thioamide **3** (1.0 mmol) in acetic acid (2.0 mL) were added the derivatives of acetylene dicarboxylic acid **5** (1.0 mmol), and the mixture was stirred at 60 °C under oil-bath heating for 3−48 h until the TLC analysis indicated total consumption of the starting thioamide **3**. The resulting mixture was cooled in an ice bath for 1 h. The precipitate was collected by filtration, washed with water (5 mL), and dried or the crude product was obtained by flash column chromatography on silica gel (eluting with methylene chloride and chloroform/ethanol = 10/1) to afford the resulting compound.

*General Procedure C (GP-C): Synthesis of 5-Oxothiazolidin-4-ylidenes **9a**−**d**.* Acetylene dicarboxylic acid or ester (10.0 mmol) was added to a solution of cyanothioacetamide **2** (10.0 mmol, 1.00 g) in acetic acid (10.0 mL). The mixture was stirred at 60 °C under oil-bath heating for 2−4 h until the TLC analysis indicated total consumption of the starting cyanothioacetamide **2**. The resulting mixture was diluted with water (15 mL) and cooled in an ice bath for 1 h. The precipitate was filtrated, washed with water (20 mL), and dried.

*General Procedure D (GP-D): Synthesis of the DTPs **8k**−**o**.* A mixture of thiazolidinone **9** (1.0 mmol), aldehyde **1** (1.0 mmol), and AcONa (2.0 mmol, 0.164 g) in acetic acid (2.0 mL) was stirred at 118 °C under oil-bath heating for 14−18 h until the TLC analysis indicated total consumption of the starting thiazolidinone **9** and aldehyde **1**. The reaction mixture was poured into crushed ice and allowed to stand for 1 h. The precipitate was collected by filtration, washed with water (5 mL), and dried. Then the crude product was purified by flash column chromatography on silica gel (eluting with hexane/ethyl acetate = 3/2) to afford the resulting compound.

*General Procedure E (GP-E): Synthesis of the 4H,6H-Pyrido[2,1-b][1,3]thiazine **12a**.* To a solution of thioamide **3a** (1.0 mmol, 0.214 g) in acetic acid (2.0 mL) was added methyl propiolate (1.0 mmol, 0.088 mL), and the mixture was stirred at 60 °C under oil-bath heating until the TLC analysis indicated total consumption of the starting thioamide **3**. The resulting mixture was cooled in an ice bath for 1 h. The precipitate was collected by filtration and washed with water (5 mL).

*General Procedure F (GP-F): Synthesis of the 4H,6H-Pyrido[2,1-b][1,3]thiazines **12b**−**e**.* A mixture of thiazinone **10** (1.0 mmol, 0.152 g), aldehyde **1** (1.0 mmol), and AcONa (2.0 mmol, 0.164 g) in acetic acid (2.0 mL) was stirred at 118 °C under oil-bath heating for 8−20 h until the TLC analysis indicated total consumption of the starting thiazinone **10** and aldehyde **1**. The reaction mixture was poured into crushed ice and allowed to stand for 1 h. The precipitate was collected by filtration, washed with water (5 mL), and dried. Then the crude product was purified by flash column chromatography on silica gel (eluting with hexane/ethyl acetate = 3/2) to afford the resulting compound.

*2-Cyano-5-phenylpenta-2,4-dienethioamide (**3a**):* Prepared according to GP-A; orange powder (2.033 g, 95% yield); mp = 166−167 °C; ^{1}H NMR (DMSO-d_6, 400 MHz) δ 9.96 (br s, 1H), 9.45 (br s, 1H), 7.97 (d, 1H, J = 11.2 Hz), 7.71 (m, 2H), 7.47 (m, 4H), 7.17 (dd, 1H, J = 11.2, J = 15.4 Hz); ^{13}C{^{1}H} NMR (DMSO-d_6, 100 MHz, APT) δ (+) 191.6, (−) 148.3, (−) 148.1, (+) 135.5, (−) 131.2, (−) 129.7, (−) 128.7, (−) 123.9, (+) 115.6, (+) 113.9; FT-IR (neat) ν_{max} (cm^{-1}) 3342, 3266, 3154, 2221, 1605; MS-EI, m/z 214 (M$^+$, 100%). Anal. Calcd for $C_{12}H_{10}N_2S$: C, 67.26; H, 4.70; N, 13.07. Found: C, 67.17; H, 4.77; N, 13.18.

*2-Cyano-5-(4-methoxyphenyl)penta-2,4-dienethioamide (**3b**):* Prepared according to GP-A; orange powder (1.830 g, 75% yield); mp = 193−195 °C; ^{1}H NMR (DMSO-d_6, 400 MHz) δ δ 9.86 (br s, 1H), 9.34 (br s), 7.97 (d, 1H, J = 11.3 Hz), 7.67 (d, 2H, J = 8.8 Hz), 7.43 (d, 1H, J = 15.2 Hz), 7.02 (m, 3H), 3.82 (s, 3H); ^{13}C{^{1}H} NMR (DMSO-d_6, 100 MHz, APT) δ (+) 191.2, (+) 161.5, (−) 148.8, (−) 147.9, (−) 130.3, (+) 127.7, (−) 121.1, (+) 115.4, (−) 114.7, (+) 111.7, (−) 55.4; FT-IR ν_{max} (cm^{-1}) 3388, 3320, 3222, 2214, 1644; MS-EI, m/z 244 (M$^+$, 100%). Anal. Calcd for $C_{13}H_{12}N_2OS$: C, 63.91; H, 4.95; N, 11.47. Found: C, 63.69; H, 4.97; N, 11.42.

*2-Cyano-5-(4-(dimethylamino)phenyl)penta-2,4-dienethioamide (**3c**):* Prepared according to GP-A; dark red powder (2.107 g, 82% yield); mp = 230−232 °C; ^{1}H NMR (DMSO-d_6, 400 MHz) δ 9.67 (br s, 1H), 9.13 (br s, 1H), 7.98 (d, 1H, J = 11.5 Hz), 7.51 and 6.72 (AA′XX′, 4H, J = 8.9 Hz), 7.34 (d, 1H, J = 14.9 Hz), 6.88 (dd, 1H, J = 14.9, J = 11.6 Hz), 3.00 (s, 6H); ^{13}C{^{1}H} NMR (DMSO-d_6, 100 MHz) δ 191.4, 152.2, 150.1, 149.7, 130.5, 122.4, 117.7, 116.0, 111.9, 108.5; FT-IR (neat) ν_{max} (cm^{-1}) 3344, 3273, 3154, 2217, 1634; MS-EI, m/z 257 (M$^+$, 100%). Anal. Calcd for $C_{14}H_{15}N_3S$: C, 65.34; H, 5.88; N, 16.33. Found: C, 65.51; H, 6.03; N, 16.46.

*2-Cyano-5-(2-methoxyphenyl)penta-2,4-dienethioamide (**3d**):* Prepared according to GP-A; orange powder (0.586 g, 24% yield); mp = 133−135 °C; ^{1}H NMR (DMSO-d_6, 400 MHz) δ 9.87 (br s, 1H), 9.34 (br s, 1H), 7.97 (d, 1H, J = 11.3 Hz), 7.66 (d, 1H, J = 7.1 Hz), 7.60 (d, 1H, J = 15.4 Hz), 7.42 (t, 1H, J = 7.3 Hz), 7.25 (dd, 1H, J = 15.4, J = 11.4 Hz), 7.09 (d, 1H, J = 8.3 Hz), 7.01 (t, 1H, J = 7.5 Hz), 3.87 (s, 3H); ^{13}C{^{1}H} NMR (DMSO-d_6, 100 MHz) δ 191.2, 158.0, 148.4, 142.9, 132.4, 128.9, 124.3, 123.4, 121.0, 115.3, 112.8, 111.9, 55.7; FT-IR (neat) ν_{max} (cm^{-1}) 3413, 3273, 3167, 2200, 1629; MS-EI, m/z 244 (M$^+$, 100%). Anal. Calcd for $C_{13}H_{12}N_2OS$: C, 63.91; H, 4.95; N, 11.47. Found: C, 63.79; H, 4.96; N, 11.43.

*6-Amino-3-methyl-2-phenyl-2H-thiopyran-5-carbonitrile (**4**):* Prepared according to GP-A; yellow powder (1.664 g, 73% yield); mp = 130−132 °C; ^{1}H NMR (DMSO-d_6, 400 MHz) δ 7.31 (m, 5H), 6.95 (s, 2H), 5.98 (d, 1H, J = 1.4 Hz), 4.73 (s, 1H), 1.74 (d, 3H, J = 1.2 Hz); ^{13}C{^{1}H} NMR (DMSO-d_6, 100 MHz) δ 154.3, 140.7, 128.6, 127.6, 127.1, 120.7, 119.4, 119.3, 72.4, 46.7, 21.5; FT-IR (neat) ν_{max} (cm^{-1}) 3401, 3300, 3206, 3154, 2180, 1616; MS-EI, m/z 228 (M$^+$, 100%). Anal. Calcd for $C_{13}H_{12}N_2S$: C, 68.39; H, 5.30; N, 12.27. Found: C, 68.63; H, 5.38; N, 12.37.

*Methyl-2-(8-cyano-3-oxo-5-phenyl-5H-thiazolo[3,2-a]pyridin-2(3H)-ylidene)acetate (**8a**):* Prepared according to GP-B; after column chromatography (methylene chloride), an orange powder (0.253 mg, 78% yield) was obtained; mp = 178−180 °C; ^{1}H NMR (DMSO-d_6, 400 MHz) δ 7.35 (m, 5H), 6.78 (s, 1H), 6.23 (dd, 1H, J = 9.8, 1.5 Hz), 6.02 (dd, 1H, J = 4.5, 1.4 Hz), 5.90 (dd, 1H, J = 9.8, 4.6 Hz), 3.81 (s, 3H); ^{13}C{^{1}H} NMR (DMSO-d_6, 100 MHz) δ 166.2, 163.1, 147.4, 139.1, 138.4, 128.9, 128.4, 126.7, 123.3, 116.2, 116.1, 115.3, 84.1, 58.1, 52.8; FT-IR (neat) ν_{max} (cm^{-1}) 3071, 2993, 2947, 2894, 2845, 2213, 1705, 1685 (CO); HRMS (ESI-TOF) m/z [M + H]$^+$ calcd for $C_{17}H_{12}N_2O_3SH$ 325.0641; found 325.0643; [M + Na]$^+$ calcd for $C_{17}H_{12}N_2O_3SNa$ 347.0461; found 347.0463; [M + K]$^+$ calcd for $C_{17}H_{12}N_2O_3SK$ 363.0200; found 363.0204.

https://dx.doi.org/10.1021/acs.joc.0c01934
J. Org. Chem. XXXX, XXX, XXX−XXX

*Methyl-2-(8-cyano-5-(4-methoxyphenyl)-3-oxo-5H-thiazolo[3,2-a]pyridin-2(3H)-ylidene)acetate (**8b**):* Prepared according to GP-B; after column chromatography (methylene chloride), an orange powder (0.234 mg, 66% yield) was obtained; mp = 169−171 °C; ^{1}H NMR (DMSO-d_6, 400 MHz) δ 7.28 and 6.92 (AA′XX′, 4H, J = 8.5 Hz), 6.76 (s, 1H), 6.24 (d, 1H, J = 9.8 Hz), 5.97 (d, 1H, J = 4.0 Hz), 5.86 (dd, 1H, J = 9.8, 4.6 Hz), 3.80 (s, 3H), 3.74 (s, 3H); ^{13}C{^{1}H} NMR (DMSO-d_6, 100 MHz) δ 165.8, 162.8, 159.3, 146.7, 138.1, 130.7, 128.2, 122.9, 116.1, 115.7, 115.1, 114.1, 84.0, 57.3, 54.9, 52.4; FT-IR (neat) ν_{max} (cm^{-1}) 3070, 3043, 3014, 2960, 2839, 2218, 1713, 1683; HRMS (ESI-TOF) m/z [M + H]$^+$ calcd for $C_{18}H_{14}N_2O_4SH$ 355.0747; found 355.0744; [M + Na]$^+$ calcd for $C_{18}H_{14}N_2O_4SNa$ 377.0566; found 377.0570; [M + K]$^+$ calcd for $C_{18}H_{14}N_2O_4SK$ 393.0306; found 393.0301.

*Methyl-2-(8-cyano-5-(4-(dimethylamino)phenyl)-3-oxo-5H-thiazolo[3,2-a]pyridin-2(3H)-ylidene)acetate (**8c**):* Prepared according to GP-B; after column chromatography (methylene chloride), an orange powder (0.184 mg, 50% yield) was obtained; mp = 210−212 °C; ^{1}H NMR (DMSO-d_6, 400 MHz) δ 7.14 and 6.67 (AA′XX′, 4H, J = 7.6 Hz), 6.75 (s, 1H), 6.23 (d, 1H, J = 9.6 Hz), 5.88 (d, 1H, J = 4.1 Hz), 5.84 (dd, 1H, J = 9.6 Hz, J = 4.0 Hz), 3.80 (s, 3H), 2.88 (s, 6H); ^{13}C{^{1}H} NMR (DMSO-d_6, 100 MHz) δ 165.7, 162.8, 150.3, 146.5, 138.2, 127.8, 125.6, 123.1, 115.9, 115.7, 114.9, 112.0, 84.0, 57.5, 52.4, 39.6; FT-IR (neat) ν_{max} (cm^{-1}) 3066, 2954, 2888, 2803, 2217, 1707; HRMS (ESI-TOF) m/z [M + H]$^+$ calcd for $C_{19}H_{17}N_3O_3SH$ 368.1063; found 368.1069; [M + Na]$^+$ calcd for $C_{19}H_{17}N_3O_3SNa$ 390.0883; found 390.0874; [M + K]$^+$ calcd for $C_{19}H_{17}N_3O_3SK$ 406.0622; found 406.0618.

*Methyl-2-(8-cyano-5-(2-methoxyphenyl)-3-oxo-5H-thiazolo[3,2-a]pyridin-2(3H)-ylidene)acetate (**8d**):* Prepared according to GP-B; after column chromatography (methylene chloride), an orange powder (0.134 mg, 38% yield) was obtained; mp = 182−184 °C; ^{1}H NMR (DMSO-d_6, 400 MHz) δ 7.30 (t, 1H, J = 7.8 Hz), 7.10 (dd, 1H, J = 7.5 Hz, J = 1.0 Hz), 7.06 (d, 1H, J = 8.2 Hz), 6.94 (t, 1H, J = 7.4 Hz), 6.75 (s, 1H), 6.17 (dd, 1H, J = 4.2 Hz, J = 0.9 Hz), 6.14 (dd, 1H, J = 9.9 Hz, J = 1.3 Hz), 5.79 (dd, 1H, J = 9.8, 4.5 Hz), 3.81 (s, 6H); ^{13}C{^{1}H} NMR (DMSO-d_6, 100 MHz) δ 166.7, 163.3, 156.4, 148.3, 138.9, 130.1, 127.4, 127.2, 122.4, 121.5, 116.8, 116.6, 115.5, 112.2, 84.5, 56.2, 55.1, 53.3; FT-IR (neat) ν_{max} (cm^{-1}) 3064, 2995, 2947, 2837, 2207, 1710, 1689; HRMS (ESI-TOF) m/z [M + H]$^+$ calcd for $C_{18}H_{14}N_2O_4SH$ 355.0747; found 355.0753; [M + Na]$^+$ calcd for $C_{18}H_{14}N_2O_4SNa$ 377.0566; found 377.0566; [M + K]$^+$ calcd for $C_{18}H_{14}N_2O_4SK$ 393.0306; found 393.0315.

*Ethyl-2-(8-cyano-3-oxo-5-phenyl-5H-thiazolo[3,2-a]pyridin-2(3H)-ylidene)acetate (**8e**):* Prepared according to GP-B; after column chromatography (methylene chloride), an orange powder (0.152 mg, 45% yield) was obtained; mp = 191−193 °C; ^{1}H NMR (DMSO-d_6, 400 MHz) δ 7.35 (m, 5H), 6.75 (s, 1H), 6.23 (d, 1H, J = 9.8 Hz), 6.03 (d, 1H, J = 4.3 Hz), 5.90 (dd, 1H, J = 9.8, 4.5 Hz), 4.27 (q, 2H, J = 7.0 Hz), 1.26 (t, 3H, J = 7.1 Hz); ^{13}C{^{1}H} NMR (DMSO-d_6, 100 MHz) δ 165.5, 163.1, 147.4, 139.1, 138.2, 128.9, 128.4, 126.7, 123.2, 116.4, 115.8, 115.7, 84.2, 61.7, 58.1, 13.9; FT-IR (neat) ν_{max} (cm^{-1}) 3066, 2983, 2962, 2887, 2213, 1707, 1683; HRMS (ESI-TOF) m/z [M + H]$^+$ calcd for $C_{18}H_{14}N_2O_3SH$ 339.0798; found 339.0798; [M + Na]$^+$ calcd for $C_{18}H_{14}N_2O_3SNa$ 361.0617; found 361.0617; [M + K]$^+$ calcd for $C_{18}H_{14}N_2O_3SK$ 377.0357; found 377.0367.

*Ethyl-2-(8-cyano-5-(4-methoxyphenyl)-3-oxo-5H-thiazolo[3,2-a]pyridin-2(3H)-ylidene)acetate (**8f**):* Prepared according to GP-B; after column chromatography (methylene chloride), an orange powder (0.287 mg, 78% yield) was obtained; mp = 152−154 °C; ^{1}H NMR (DMSO-d_6, 400 MHz) δ 7.27 and 6.92 (AA′XX′, 4H, J = 8.6 Hz), 6.73 (s, 1H), 6.23 (d, 1H, J = 9.8 Hz), 5.96 (d, 1H, J = 4.4 Hz), 5.86 (dd, 1H, J = 9.8, 4.6 Hz), 4.26 (q, 2H, J = 7.0 Hz), 3.73 (s, 3H), 1.26 (t, 3H, J = 7.1 Hz); ^{13}C{^{1}H} NMR (DMSO-d_6, 100 MHz) δ 165.6, 163.1, 159.3, 147.2, 138.4, 130.9, 128.5, 123.2, 116.2, 116.1, 115.5, 114.2, 84.0, 61.7, 57.5, 55.1, 13.9; FT-IR (neat) ν_{max} (cm^{-1}) 3063, 2992, 2960, 2904, 2838, 2211, 1705, 1683; HRMS (ESI-TOF) m/z [M + H]$^+$ calcd for $C_{19}H_{18}N_2O_4SH$ 369.0904; found 369.0905; HRMS (ESI-TOF) m/z [M + H]$^+$ calcd for $C_{19}H_{16}N_2O_4SH$ 369.0904; found 369.0905; [M + Na]$^+$ calcd for $C_{19}H_{16}N_2O_4SNa$ 391.0723; found 391.0726; [M + K]$^+$ calcd for $C_{19}H_{16}N_2O_4SK$ 407.0462; found 407.0460.

*Ethyl-2-(8-cyano-5-(4-(dimethylamino)phenyl)-3-oxo-5H-thiazolo[3,2-a]pyridin-2(3H)-ylidene)acetate (**8g**):* Prepared according to GP-B; after column chromatography (methylene chloride), an orange powder (0.114 mg, 30% yield) was obtained; mp = 181−183 °C; ^{1}H NMR (DMSO-d_6, 400 MHz) δ 7.14 and 6.67 (AA′XX′, 4H, J = 8.7 Hz), 6.72 (s, 1H), 6.23 (d, 1H, J = 9.7 Hz), 5.88 (d, 1H, J = 5.0 Hz), 5.84 (dd, 1H, J = 9.6 Hz, J = 4.7 Hz), 4.26 (q, 2H, J = 7.0 Hz), 2.87 (s, 6H), 1.26 (t, 3H, J = 7.1 Hz); ^{13}C{^{1}H} NMR (DMSO-d_6, 100 MHz) δ 165.5, 163.1, 150.6, 146.8, 138.3, 128.0, 125.9, 123.4, 116.2, 115.9, 115.6, 112.3, 99.5, 84.3, 61.7, 57.7, 13.9; FT-IR (neat) ν_{max} (cm^{-1}) 3183, 3151, 3081, 3067, 3054, 3037, 2984, 2955, 2904, 2864, 2803, 2215, 1706, 1687; HRMS (ESI-TOF) m/z [M + H]$^+$ calcd for $C_{20}H_{19}N_3O_3SH$ 382.1220; found 382.1232; [M + Na]$^+$ calcd for $C_{20}H_{19}N_3O_3SNa$ 404.1039; found 404.1038; [M + K]$^+$ calcd for $C_{20}H_{19}N_3O_3SK$ 420.0779; found 420.0775.

*Ethyl-2-(8-cyano-5-(2-methoxyphenyl)-3-oxo-5H-thiazolo[3,2-a]pyridin-2(3H)-ylidene)acetate (**8h**):* Prepared according to GP-B; after column chromatography (methylene chloride), an orange powder (0.177 mg, 48% yield) was obtained; mp = 188−190 °C; ^{1}H NMR (DMSO-d_6, 400 MHz) δ 7.30 (t, 1H, J = 7.9 Hz), 7.10 (dd, 1H, J = 7.6 Hz, J = 1.4 Hz), 7.06 (d, 1H, J = 8.2 Hz), 6.94 (t, 1H, J = 7.4 Hz), 6.73 (s, 1H), 6.17 (dd, 1H, J = 4.3 Hz, J = 1.4 Hz), 6.13 (dd, 1H, J = 9.8 Hz, J = 1.5 Hz), 5.79 (dd, 1H, J = 9.8, 4.5 Hz), 4.28 (q, 2H, J = 7.1 Hz), 3.82 (s, 3H), 1.27 (t, 3H, J = 7.1 Hz); ^{13}C{^{1}H} NMR (DMSO-d_6, 100 MHz) δ 165.3, 162.6, 155.8, 147.5, 137.9, 129.3, 126.7, 121.6, 120.7, 116.2, 115.7, 115.2, 111.6, 83.8, 61.4, 55.6, 54.4; FT-IR (neat) ν_{max} (cm^{-1}) 3066, 2996, 2970, 2938, 2838, 2204, 1709, 1688; HRMS (ESI-TOF) m/z [M + H]$^+$ calcd for $C_{19}H_{16}N_2O_4SH$ 369.0904; found 369.0911; [M + Na]$^+$ calcd for $C_{19}H_{16}N_2O_4SNa$ 391.0723; found 391.0731; [M + K]$^+$ calcd for $C_{19}H_{16}N_2O_4SK$ 407.0462; found 407.0471.

*2-(8-Cyano-3-oxo-5-phenyl-5H-thiazolo[3,2-a]pyridin-2(3H)-ylidene)acetic Acid (**8i**):* Prepared according to GP-B; after column chromatography (chloroform/ethanol = 10/1), an orange powder (0.183 mg, 59% yield) was obtained; mp = 219−221 °C; ^{1}H NMR (DMSO-d_6, 400 MHz) δ 7.34 (m, 5H), 6.71 (s, 1H), 6.21 (dd, 1H, J = 9.8, 1.2 Hz), 6.02 (d, 1H, J = 3.6 Hz), 5.88 (dd, 1H, J = 9.8, 4.6 Hz). ^{13}C{1H} NMR (DMSO-d_6, 100 MHz) δ 166.8, 163.3, 148.1, 139.2, 138.0, 128.9, 128.4, 126.7, 123.0, 116.6, 116.2, 116.1, 83.6, 58.0; FT-IR (neat) ν_{max} (cm^{-1}) 3071, 3004, 2966, 2213, 1713, 1671; HRMS (ESI-TOF) m/z [M + H]$^+$ calcd for $C_{16}H_{10}N_2O_3SH$ 311.0485; found 311.0484.

*2-(8-Cyano-5-(4-methoxyphenyl)-3-oxo-5H-thiazolo[3,2-a]-pyridin-2(3H)-ylidene)acetic Acid (**8j**):* Prepared according to GP-B; after column chromatography (chloroform/ethanol = 10/1), an orange powder (0.231 mg, 68% yield) was obtained; mp = 204−206 °C; ^{1}H NMR (DMSO-d_6, 400 MHz) δ 13.61 (br s, 1H), 7.27 and 6.92 (AA′XX′, 4H, J = 8.5 Hz), 6.69 (s, 1H), 6.21 (d, 1H, J = 9.8 Hz), 5.95 (d, 1H, J = 4.1 Hz), 5.84 (dd, 1H, J = 9.8, 4.6 Hz), 3.73 (s, 3H); ^{13}C{^{1}H} NMR (DMSO-d_6, 100 MHz) δ 166.9, 163.3, 159.3, 147.8, 137.9, 131.0, 128.5, 122.9, 116.8, 116.3, 116.2, 114.2, 83.6, 57.4, 55.1; FT-IR (neat) ν_{max} (cm^{-1}) 3049, 3006, 2974, 2883, 2853, 2833, 2216, 1709, 1670; HRMS (ESI-TOF) m/z [M + H]$^+$ calcd for $C_{17}H_{12}N_2O_4SH$ 341.0591; found 341.0592; [M + Na]$^+$ calcd for $C_{17}H_{12}N_2O_4SNa$ 363.0410; found 363.0408; [M + K]$^+$ calcd for $C_{17}H_{12}N_2O_4SK$ 379.0149; found 379.0149.

*Methyl (2-(Cyanomethylene)-5-oxothiazolidin-4-ylidene)acetate (**9a**):* Prepared according to GP-C; white powder (1.428 g, 68% yield); mp = 223−225 °C; ^{1}H NMR (DMSO-d_6, 400 MHz) δ 12.9 (br s, 1H), 6.72 and 6.66* (s, 1H); 5.44* and 5.39 (s, 1H), 3.81 and 3.78* (s, 3H); 5:1 mixture of isomers; ^{13}C{^{1}H} NMR (DMSO-d_6, 100 MHz) δ 166.1* and 166.0, 165.7* and 165.2, 154.8 and 153.5*, 142.6* and 141.8, 116.6 and 115.4*, 114.5 and 113.6*, 72.2 and 70.2*, 52.7 and 52.5*; FT-IR (neat) ν_{max} (cm^{-1}) 3155, 2965, 2820, 2224, 1730, 1682; MS-EI, m/z 210 (M$^+$, 83%). Anal. Calcd for $C_8H_6N_2O_3S$: C, 45.71; H, 2.88 2.86; N, 13.33. Found: C, 45.69; H, 2.80; N, 13.30.

*Ethyl (2-(Cyanomethylene)-5-oxothiazolidin-4-ylidene)acetate (**9b**):* Prepared according to GP-C; white powder (1.882 g, 84% yield); mp = 201−203 °C; ^{1}H NMR (DMSO-d_6, 400 MHz) δ 12.9 (br

https://dx.doi.org/10.1021/acs.joc.0c01934
J. Org. Chem. XXXX, XXX, XXX−XXX

s, 1H), 6.70 and 6.64* (s, 1H), 5.44* and 5.39 (s, 1H), 4.27 (q, 2H, J = 7.1 Hz), 1.28 (t, 3H, J = 7.1 Hz); 5:1 mixture of isomers; $^{13}C\{^1H\}$ NMR (DMSO-d_6, 100 MHz) δ 165.7* and 165.5, 165.6* and 165.2, 154.9 and 153.6*, 142.5* and 141.6, 116.6 and 115.4*, 114.8 and 114.0*, 72.1 and 70.1*, 61.6 and 61.4*, 13.9; FT-IR (neat) ν_{max} (cm^{-1}) 3156, 2981, 2931, 2828, 2208, 1729, 1683; MS-EI, m/z 224 (M^+, 98%). Anal. Calcd for $C_9H_8N_2O_3S$: C, 48.21; H, 3.60; N, 12.49. Found: C, 48.30; H, 3.50; N, 12.48.

(2-(Cyanomethylene)-5-oxothiazolidin-4-ylidene)acetic Acid ***(9c)****:* Prepared according to GP-C; white powder (1.392 g, 71% yield); mp = 276−278 °C; ^1H NMR (DMSO-d_6, 400 MHz) δ 13.19 (br s, 2H), 6.65 and 6.60* (s, 1H), 5.37* and 5.34 (s, 1H); 5:1 mixture of isomers; $^{13}C\{^1H\}$ NMR (DMSO-d_6, 100 MHz) δ 167.4* and 167.3, 166.4* and 165.9, 156.0 and 154.6*, 142.4* and 141.6, 117.3 and 116.0*, 116.6 and 115.7*, 72.2 and 70.2*; FT-IR (neat) ν_{max} (cm^{-1}) 3244, 2225, 1726, 1676; MS-EI, m/z 196 (M^+, 92%). Anal. Calcd for $C_7H_4N_2O_3S$: C, 42.86; H, 2.06; N, 14.28. Found: C, 42.72; H, 2.04; N, 14.18.

Methyl-2-(8-cyano-6-methyl-3-oxo-5-phenyl-5H-thiazolo[3,2-a]-pyridin-2(3H)-ylidene)acetate ***(8k)****:* Prepared according to GP-D; after column chromatography (hexane/ethyl acetate = 3/2), a red powder (0.199 mg, 59% yield) was obtained; mp = 205−207 °C; ^1H NMR (DMSO-d_6, 400 MHz) δ 7.37 (m, 5H), 6.74 (s, 1H), 6.09 (s, 1H), 5.83 (s, 1H), 3.79 (s, 3H), 1.65 (s, 3H); $^{13}C\{^1H\}$ NMR (DMSO-d_6, 100 MHz) δ 166.2, 162.9, 144.6, 138.7, 138.3, 131.9, 128.9, 128.7, 127.4, 116.2, 114.8, 113.1, 84.5, 61.5, 52.7, 19.2; FT-IR (neat) ν_{max} (cm^{-1}) 3062, 3027, 2987, 2950, 2938, 2905, 2882, 2876, 2210, 1712, 1696; HRMS (ESI-TOF) m/z $[M + H]^+$ calcd for $C_{18}H_{14}N_2O_3SH$ 339.0798; found 339.0802; $[M + Na]^+$ calcd for $C_{18}H_{14}N_2O_3SNa$ 361.0617; found 361.0620; $[M + K]^+$ calcd for $C_{18}H_{14}N_2O_3SK$ 377.0357; found 377.0363.

Methyl-2-(8-cyano-5,6-dimethyl-3-oxo-5H-thiazolo[3,2-a]-pyridin-2(3H)-ylidene)acetate ***(8l)****:* Prepared according to GP-D; after column chromatography (hexane/ethyl acetate = 3/2), a red powder (0.061 mg, 22% yield) was obtained; mp = 194−196 °C; ^1H NMR (DMSO-d_6, 400 MHz) δ 6.82 (s, 1H), 5.93 (s, 1H), 4.91 (q, 1H, J = 6.3 Hz), 3.82 (s, 3H), 1.87 (s, 3H), 1.32 (d, 3H, J = 6.4 Hz); $^{13}C\{^1H\}$ NMR (DMSO-d_6, 100 MHz) δ 166.3, 163.2, 144.6, 139.5, 133.2, 116.1, 114.2, 113.0, 84.8, 54.0, 52.7, 19.1, 17.6; FT-IR (neat) ν_{max} (cm^{-1}) 3056, 3006, 2987, 2951, 2918, 2200, 1704; HRMS (ESI-TOF) m/z $[M + H]^+$ calcd for $C_{13}H_{12}N_2O_3SH$ 277.0641; found 277.0642; $[M + Na]^+$ calcd for $C_{13}H_{12}N_2O_3SNa$ 299.0461; found 299.0460.

Methyl-2-(8-cyano-5-methyl-3-oxo-5H-thiazolo[3,2-a]pyridin-2(3H)-ylidene)acetate ***(8m)****:* Prepared according to GP-D; after column chromatography (hexane/ethyl acetate = 3/2), an orange powder (39 mg, 15% yield) was obtained; mp = 182−184 °C; ^1H NMR (DMSO-d_6, 400 MHz) δ 6.83 (s, 1H), 6.12 (dd, 1H, J = 9.9 Hz, J = 1.3 Hz), 5.84 (dd, 1H, J = 9.9 Hz, J = 4.5 Hz), 5.03 (m, 1H), 3.82 (s, 3H), 1.32 (d, 3H, J = 6.5 Hz); $^{13}C\{^1H\}$ NMR (DMSO-d_6, 100 MHz) δ 166.7, 163.9, 148.1, 139.7, 124.9, 117.2, 116.6, 115.1, 84.5, 53.3, 51.6, 20.2; FT-IR (neat) ν_{max} (cm^{-1}) 3049, 2928, 2851, 2206, 1711; HRMS (ESI-TOF) m/z $[M + H]^+$ calcd for $C_{12}H_{10}N_2O_3SH$ 263.0485; found 263.0487.

Ethyl-2-(8-cyano-6-methyl-3-oxo-5-phenyl-5H-thiazolo[3,2-a]-pyridin-2(3H)-ylidene)acetate ***(8n)****:* Prepared according to GP-D; after column chromatography (hexane/ethyl acetate = 3/2), an orange powder (0.120 mg, 34% yield) was obtained; mp = 189−191 °C; ^1H NMR (DMSO-d_6, 400 MHz) δ 7.37 (m, 5H), 6.69 (s, 1H), 6.07 (s, 1H), 5.82 (s, 1H), 4.25 (q, 2H, J = 7.1 Hz), 1.66 (s, 3H), 1.25 (t, 3H, J = 7.1 Hz); $^{13}C\{^1H\}$ NMR (DMSO-d_6, 100 MHz) δ 165.6, 162.9, 144.6, 138.6, 138.2, 131.8, 128.8, 128.7, 127.4, 116.0, 115.2, 113.2, 84.6, 61.7, 61.5, 19.2, 13.9; FT-IR (neat) ν_{max} (cm^{-1}) 3079, 2983, 2208, 1703, 1686; HRMS (ESI-TOF) m/z $[M + H]^+$ calcd for $C_{19}H_{16}N_2O_3SH$ 353.0954; found 353.0962; $[M + Na]^+$ calcd for $C_{19}H_{16}N_2O_3SNa$ 375.0774; found 375.0773; $[M + K]^+$ calcd for $C_{19}H_{16}N_2O_3SK$ 391.0513; found 391.0518.

Ethyl-2-(8-cyano-5,6-dimethyl-3-oxo-5H-thiazolo[3,2-a]pyridin-2(3H)-ylidene)acetate ***(8o)****:* Prepared according to GP-D; after column chromatography (hexane/ethyl acetate = 3/2), an orange powder (0.075 mg, 26% yield) was obtained; mp = 141−143 °C; ^1H NMR (DMSO-d_6, 400 MHz) δ 6.77 (s, 1H), 5.92 (s, 1H), 4.90 (q, 1H, J = 6.2 Hz), 4.28 (q, 2H, J = 7.1 Hz), 1.87 (s, 3H), 1.32 (d, 3H, J = 6.5 Hz), 1.28 (t, 3H, J = 7.1 Hz); $^{13}C\{^1H\}$ NMR (DMSO-d_6, 100 MHz) δ 168.8, 163.2, 144.6, 139.4, 133.2, 116.1, 114.4, 113.1, 84.8, 61.7, 54.0, 19.1, 17.6, 14.0; FT-IR (neat) ν_{max} (cm^{-1}) 3076, 2985, 2957, 2922, 2852, 2206, 1701, 1690; HRMS (ESI-TOF) m/z $[M + H]^+$ calcd for $C_{14}H_{14}N_2O_3SH$ 291.0798; found 291.0803; $[M + Na]^+$ calcd for $C_{14}H_{14}N_2O_3SNa$ 313.0617; found 313.0622.

(4-Oxo-3,4-dihydro-2H-1,3-thiazin-2-ylidene)acetonitrile ***(10)****:* Methyl propiolate (10.0 mmol, 0.889 mL) was added to a solution of cyanothioacetamide **2** (10.0 mmol, 1.000 g) in acetic acid (10.0 mL). The mixture was stirred at 118 °C under oil-bath heating for 3 h until the TLC analysis indicated total consumption of the starting cyanothioacetamide **2**. The resulting mixture was diluted with water and cooled in an ice bath for 1 h. The precipitate was collected by filtration, washed with water (20 mL), and dried to obtain a brown powder (0.866 g, 57% yield); mp = 187−189 °C; ^1H NMR (DMSO-d_6, 400 MHz) δ 11.63 (s, 1H), 7.69 and 6.22 (AX, 2H, J = 10.4 Hz), 4.89 (s, 1H); $^{13}C\{^1H\}$ NMR (DMSO-d_6, 100 MHz) δ 159.8, 154.2, 136.7, 117.1, 116.8, 68.7; FT-IR (neat) ν_{max} (cm^{-1}) 3516, 2198, 1685; MS-EI, m/z 152 (M^+, 65%). Anal. Calcd for $C_6H_4N_2OS$: C, 47.36; H, 2.65; N, 18.41. Found: C, 47.41; H, 2.67; N, 18.20.

4-Oxo-6-phenyl-4H,6H-pyrido[2,1-b][1,3]thiazine-9-carbonitrile ***(12a)****:* Prepared according to GP-E; yellow powder (0.162 mg, 62% yield); mp = 165−166 °C; ^1H NMR (DMSO-d_6, 400 MHz) δ 7.75 and 6.39 (AX, 2H, J = 10.4 Hz), 7.35 (m, 5H), 6.52 (d, 1H, J = 6.0 Hz), 6.19 (d, 1H, J = 9.6 Hz), 5.30 (dd, 1H, J = 9.6 Hz, J = 5.9 Hz); $^{13}C\{^1H\}$ NMR (DMSO-d_6, 100 MHz) δ 159.2, 146.1, 140.1, 135.8, 128.9, 128.3, 126.2, 121.1, 118.4, 118.1, 116.7, 53.0; FT-IR (neat) ν_{max} (cm^{-1}) 3056, 2926, 2200, 1675; HRMS (ESI-TOF) m/z $[M + H]^+$ calcd for $C_{15}H_{10}N_2OSH$ 267.0587; found 267.0590; $[M + Na]^+$ calcd for $C_{15}H_{10}N_2OSNa$ 289.0406; found 289.0408; $[M + K]^+$ calcd for $C_{15}H_{10}N_2OSK$ 305.0145; found 305.0147.

6-(4-Methoxyphenyl)-4-oxo-4H,6H-pyrido[2,1-b][1,3]thiazine-9-carbonitrile ***(12b)****:* Prepared according to GP-F; after column chromatography (hexane/ethyl acetate = 3/2), a yellow powder (44 mg, 15% yield) was obtained; mp = 173−175 °C; ^1H NMR (DMSO-d_6, 400 MHz) δ 7.72 and 6.38 (AX, 2H, J = 10.4 Hz), 7.28 and 6.94 (AA′XX′, 4H, J = 8.7 Hz), 6.47 (d, 1H, J = 5.9 Hz), 6.22 (d, 1H, J = 9.6 Hz), 5.77 (dd, 1H, J = 9.6, 6.0 Hz), 3.74 (s, 3H); $^{13}C\{^1H\}$ NMR (DMSO-d_6, 100 MHz) δ 159.3, 159.2, 145.7, 135.6, 131.9, 128.1, 121.1, 118.3, 118.1, 116.8, 114.2, 86.8, 55.1, 52.3; FT-IR (neat) ν_{max} (cm^{-1}) 3066, 3008, 2963, 2944, 2931, 2907, 2891, 2871, 2856, 2804, 2199, 1668; HRMS (ESI-TOF) m/z $[M + H]^+$ calcd for $C_{16}H_{12}N_2O_2SH$ 297.0692; found 297.0698; $[M + Na]^+$ calcd for $C_{16}H_{12}N_2O_2SNa$ 319.0512; found 319.0514; $[M + K]^+$ calcd for $C_{16}H_{12}N_2O_2SK$ 335.0251; found 335.0248.

7-Methyl-4-oxo-6-phenyl-4H,6H-pyrido[2,1-b][1,3]thiazine-9-carbonitrile ***(12c)****:* Prepared according to GP-F; after column chromatography (hexane/ethyl acetate = 3/2), a yellow powder (129 mg, 46% yield) was obtained; mp = 174−176 °C; ^1H NMR (DMSO-d_6, 400 MHz) δ 7.68 and 6.33 (AX, 2H, J = 10.3 Hz), 7.39 (m, 5H), 6.27 (s, 1H), 6.04 (s, 1H), 1.71 (s, 3H); $^{13}C\{^1H\}$ NMR (DMSO-d_6, 100 MHz) δ 159.2, 142.7, 138.8, 135.7, 130.3, 128.9, 128.8, 127.1, 117.9, 116.8, 114.4, 87.4, 57.2, 19.8; FT-IR (neat) ν_{max} (cm^{-1}) 3086, 3055, 3028, 3007, 2983, 2911, 2194, 1667; HRMS (ESI-TOF) m/z $[M + H]^+$ calcd for $C_{16}H_{12}N_2OSH$ 281.0743; found 281.0742.

6,7-Dimethyl-4-oxo-4H,6H-pyrido[2,1-b][1,3]thiazine-9-carbonitrile ***(12d)****:* Prepared according to GP-F; after column chromatography (hexane/ethyl acetate = 3/2), a yellow powder (72 mg, 33% yield) was obtained; mp = 161−163 °C; ^1H NMR (DMSO-d_6, 400 MHz) δ 7.70 and 6.36 (AX, 2H, J = 10.4 Hz), 5.79 (d, 1H, J = 1.3 Hz), 5.26 (q, 1H, J = 6.5 Hz), 1.81 (s, 3H), 1.14 (d, 3H, J = 6.5 Hz); $^{13}C\{^1H\}$ NMR (DMSO-d_6, 100 MHz) δ 158.9, 142.2, 135.4, 131.8, 118.2, 116.9, 113.7, 87.4, 50.1, 19.4, 16.9; FT-IR (neat) ν_{max} (cm^{-1}) 3061, 2970, 2959, 2940, 2927, 2914, 2889, 2872, 2197, 1694; HRMS (ESI-TOF) m/z $[M + H]^+$ calcd for $C_{11}H_{10}N_2OSH$ 219.0587; found 219.0584.

6-Methyl-4-oxo-4H,6H-pyrido[2,1-b][1,3]thiazine-9-carbonitrile ***(12e)****.* Prepared according to GP-F; after column chromatography (hexane/ethyl acetate = 3/2), an orange powder (31 mg, 15% yield)

https://dx.doi.org/10.1021/acs.joc.0c01934
J. Org. Chem. XXXX, XXX, XXX−XXX

was obtained; mp = 111−113 °C; ^{1}H NMR (DMSO-d_6, 400 MHz) δ 7.73 and 6.39 (AX, 2H, J = 10.4 Hz), 6.02 (d, 1H, J = 9.6 Hz), 5.63 (dd, 1H, J = 9.6 Hz, J = 5.8 Hz), 5.44 (m, 1H), 1.13 (d, 3H, J = 6.5 Hz); ^{13}C{^{1}H} NMR (DMSO-d_6, 100 MHz) δ 159.4, 146.2, 135.9, 122.7, 118.8, 118.7, 117.5, 86.8, 47.2, 19.9; FT-IR (neat) ν_{max} (cm^{-1}) 3062, 2923, 2861, 2197, 1666; HRMS (ESI-TOF) m/z [M + H]$^+$ calcd for $C_{10}H_8N_2OSH$ 205.0430; found 205.0434.

■ ASSOCIATED CONTENT

Supporting Information

The Supporting Information is available free of charge at https://pubs.acs.org/doi/10.1021/acs.joc.0c01934.

Copies of NMR spectra for new compounds; XRD crystal data; details of photophysical investigations, quantum mechanical calculations, biological investigations, and the coordinates of compounds optimized at the B3LYP/6-31G** level (PDF)

Accession Codes

CCDC 2015841−2015843 contain the supplementary crystallographic data for this paper. These data can be obtained free of charge via www.ccdc.cam.ac.uk/data_request/cif, or by emailing data_request@ccdc.cam.ac.uk, or by contacting The Cambridge Crystallographic Data Centre, 12 Union Road, Cambridge CB2 1EZ, UK; fax: +44 1223 336033.

■ AUTHOR INFORMATION

Corresponding Authors

Nataliya P. Belskaya − *Ural Federal University, Yekaterinburg 620002, Russian Federation; Postovsky Institute of Organic Synthesis, Ural Branch of Russian Academy of Science, Yekaterinburg 620219, Russian Federation;* orcid.org/0000-0002-2509-7916; Email: n.p.belskaya@urfu.ru

Enrico Benassi − *Shihezi University, Shihezi, Xinjiang 832000, China;* orcid.org/0000-0002-4614-1568; Email: ebenassi3@gmail.com

Authors

Aleksey A. Gagarin − *Ural Federal University, Yekaterinburg 620002, Russian Federation*

Polina O. Suntsova − *Ural Federal University, Yekaterinburg 620002, Russian Federation*

Artem S. Minin − *Ural Federal University, Yekaterinburg 620002, Russian Federation; M. N. Mikheev Institute of Metal Physics, Ural Branch of Russian Academy of Science, Yekaterinburg 620219, Russian Federation;* orcid.org/0000-0003-3305-3195

Varvara A. Pozdina − *Institute of Immunology and Physiology, Ekaterinburg 620049, Russian Federation*

Pavel A. Slepukhin − *Postovsky Institute of Organic Synthesis, Ural Branch of Russian Academy of Science, Yekaterinburg 620219, Russian Federation*

Complete contact information is available at: https://pubs.acs.org/10.1021/acs.joc.0c01934

Notes

The authors declare no competing financial interest.

■ ACKNOWLEDGMENTS

We thank Russian Science Foundation for financially supporting this work through Project 20-13-00089. E.B. thanks the Bingtuan Oasis Foreign Expert fund. This work was performed using the equipment of the Shared Research Center of Scientific Equipment SRC IIP UrB RAS. We also gratefully acknowledge the Siberian Branch of the Russian Academy of Sciences (SB RAS) Siberian Supercomputer Centre for providing supercomputer facilities.

■ REFERENCES

(1) Gao, X.; Liu, J.; Zuo, X.; Feng, X.; Gao, Y. Recent Advances in Synthesis of Benzothiazole Compounds Related to Green Chemistry. *Molecules* **2020**, *25*, 1675.

(2) Belskaya, N. P.; Kostova, I.; Fan, Z. Thiazole cores as organic fluorescent units: Synthesis and fluorescence. *Targets in Heterocyclic Systems* **2019**, *23*, 116−142.

(3) Bakulev, V.; Shafran, Y.; Dehaen, W. Progress in intermolecular and intramolecular reactions of thioamides with diazo compounds and azides. *Tetrahedron Lett.* **2019**, *60*, 513−523.

(4) Dyachenko, V. D.; Dyachenko, I. V.; Nenajdenko, V. G. One-Pot Synthesis of Thieno[2,3-*b*]pyridine and Pyrido[3′,2′:4,5]thieno[3,2-*d*]pyrimidine Derivatives. *Russ. Chem. Rev.* **2018**, *87*, 1−27.

(5) Belskaya, N. P.; Dehaen, W.; Bakulev, V. A. Synthesis and properties of hydrazones bearing amide, thioamide and amidine functions. *ARKIVOC* **2010**, *2010*, 275−332.

(6) Britsun, V. N.; Lozinskii, M. O. Cycloacylation of thioamides and their derivatives by compounds containing an activated multiple bond. *Chem. Heterocycl. Compd.* **2007**, *43*, 1083−1110.

(7) Danilkina, N. A.; Mikhailov, L. E.; Ivin, B. A. Condensations of thioamides with acetylenecarboxylic acid derivatives. *Russ. J. Org. Chem.* **2006**, *42*, 783−814.

(8) Jagodzinski, T. S. Thioamides as Useful Synthons in the Synthesis of Heterocycles. *Chem. Rev.* **2003**, *103*, 197−228.

(9) Suntsova, P. O.; Eltyshev, A. K.; Pospelova, T. A.; Slepukhin, P. A.; Benassi, E.; Belskaya, N. P. Design and synthesis of disubstituted and trisubstituted thiazoles as multifunctional fluorophores with large Stokes shifts. *Dyes Pigm.* **2019**, *166*, 60−71.

(10) Witalewska, M.; Wrona-Piotrowicz, A.; Zakrzewski, J. *N*-ethoxycarbonylpyrene- and perylene thioamides as building blocks in the synthesis of efficient color-tunable 4-hydroxythiazole-based fluorophores. *Dyes Pigm.* **2019**, *160*, 923−929.

(11) Liu, C.; Wu, S.; Xu, J.; Chen, L.; Zheng, P.; Chi, Y. R. Carbene-Catalyzed Enantioselective Addition of Thioamides to Bromoenals for Access to Thiazinone Heterocycles. *Org. Lett.* **2019**, *21*, 9493−9496.

(12) Ghosh, A.; Barik, S.; Biju, A. T. NHC-Catalyzed [3 + 3] Annulation of Thioamides and Modified Enals for the Enantioselective Synthesis of Functionalized Thiazinones. *Org. Lett.* **2019**, *21*, 8598−8602.

(13) Murai, T.; Yoshihara, M.; Yamaguchi, K.; Minoura, M. 2-(2-Hydroxyphenyl)-5-aminothiazoles: Synthesis and Properties Involving Dual Emissions. *Asian. Asian J. Org. Chem.* **2019**, *8*, 1102−1106.

(14) Voznesenskaia, N. G.; Shmatova, O. I.; Ilyin, M. M.; Ilyin, M. M., Jr.; Nenajdenko, V. G. Enantioselective Synthesis of Thiazole-Derived α-Perfluoroalkylated 5−7-Membered Amines. *Eur. J. Org. Chem.* **2019**, *2019*, 1893−1903.

(15) Lugovik, K. I.; Popova, A. V.; Eltyshev, A. K.; Benassi, E.; Belskaya, N. P. Synthesis of Thiazoles Bearing Aryl Enamine/Azaenamine Side Chains: Effect of the π-Conjugated Spacer Structure and Hydrogen Bonding on Photophysical Properties. *Eur. J. Org. Chem.* **2017**, *2017*, 4175−4187.

(16) El-Sheref, E. M.; Brown, A. B. Utility of Acetylenedicarboxylate in Organic Synthesis. *J. Heterocycl. Chem.* **2017**, *54*, 825−843.

(17) Bell, A. S.; Fishwick, C. W. G.; Reed, J. E. Generation and cycloadditions of 2-(*N*-acylamino)-1-thia-1,3-dienes part III: Control of diastereoselectivity using homochiral auxiliaries. *Tetrahedron* **1998**, *54*, 3219−3234.

(18) Arnaud, R.; Chavant, P. Y.; Molvinger, K.; Vallee, Y. Theoretical approach and first examples of *N*-acyl-thioformamides as dienophiles in the Diels-Alder reaction. *J. Chem. Soc., Chem. Commun.* **1995**, 1897−1898.

(19) Bloxham, J.; Dell, C. P. Reaction of 3-aryl-2-cyanothioacrylamides with electron-deficient alkynes: synthesis of 4-aryl-4H-thiopyrans. *J. Chem. Soc., Perkin Trans. 1* **1994**, *1*, 989−993.
(20) Egli, D. H.; Linden, A.; Heimgartner, H. 1,5-Dipolar Electrocyclizations in Reactions of α-Thioxo Ketones and α-Thioxo Thioamides with Diazo Compounds. *Helv. Chim. Acta* **2006**, *89*, 1910−1926.
(21) Egli, D. H.; Linden, A.; Heimgartner, H. 1,5-Dipolar Electrocyclizations of Thiocarbonyl Ylides Bearing C = N Groups: Reactions of *N*-[(Dimethylamino)methylene]thiobenzamide and 2-(Dimethylhydrazono)-1-phenylethane-1-thione with Diazo Compounds. *Helv. Chim. Acta* **2007**, *90*, 86−100.
(22) Medvedev, J. J.; Efimov, I. V.; Shafran, Y. M.; Suslonov, V. V.; Bakulev, V. A.; Nikolaev, V. A. Rh (II)-mediated domino [4 + 1]-annulation of α-cyanothioacetamides using diazoesters: A new entry for the synthesis of multisubstituted thiophenes. *Beilstein J. Org. Chem.* **2017**, *13*, 2569−2576.
(23) Hussaini, S. R.; Chamala, R. R.; Wang, Z. The Eschenmoser sulfide contraction method and its application in the synthesis of natural products. *Tetrahedron* **2015**, *71*, 6017−6086.
(24) Koduri, N. D.; Wang, Z.; Cannell, G.; Cooley, K.; Lemma, T. M.; Miao, K.; Nguyen, M.; Frohock, B.; Castaneda, M.; Scott, H.; Albinescu, D.; Hussaini, S. R. Enaminones via Ruthenium-Catalyzed Coupling of Thioamides and α-Diazocarbonyl Compounds. *J. Org. Chem.* **2014**, *79*, 7405−7414.
(25) Reddy, B. V. S.; Babu, R. A.; Ramana Reddy, M.; Reddy, B. J. M.; Sridhar, B. Intramolecular C-O/C-S bond insertion of α-diazoesters for the synthesis of 2-aryl-4*H*-benzo[*d*][1,3]oxazine and 2-aryl-4*H*-benzo-[*d*][1,3]thiazine derivatives. *RSC Adv.* **2014**, *4*, 44629−44633.
(26) Heravi, M. M.; Alishiri, T. Chapter One - Dimethyl Acetylenedicarboxylate as a Building Block in Heterocyclic Synthesis. *Adv. Heterocycl. Chem.* **2014**, *113*, 1−66.
(27) Anand, S. A. A.; Loganathan, C.; Thomas, N. S.; Saravanan, K.; Alphonsa, A. T.; Kabilan, S. Synthesis, structure prediction, pharmacokinetic properties, molecular docking and antitumor activities of some novel thiazinone derivatives. *New J. Chem.* **2015**, *39*, 7120−7129.
(28) Barnish, I. T.; Fishwick, C. W.G.; Hill, D. R.; Szanta, C. Generation and cycloadditions of 2-(*N*-Acylamino)-1-thia-1,3-dienes. Part II. Rationalization of reactivity using an FMO approach. *Tetrahedron* **1989**, *45*, 7879−7898.
(29) Belskaya, N. P.; Lugovik, K. I.; Ivina, A. D.; Bakulev, V. A.; Fan, Z. J. Reaction of enamines and azaenamines containing a thioamide group with dimethyl acetylenedicarboxylate. *Chem. Heterocycl. Compd.* **2014**, *50*, 888−900.
(30) Deryabina, T. G.; Demina, M. A.; Belskaya, N. P.; Bakulev, V. A. Reaction of 3-aryl-2-cyanothioacrylamides with dimethyl acetylenecarboxylate, methyl propiolate, and *N*-phenylmaleimide. *Russ. Chem. Bull.* **2005**, *54*, 2880−2889.
(31) Berseneva, V. S.; Tkachev, A. V.; Morzherin, Y. Y.; Dehaen, W.; Luyten, I.; Toppet, S.; Bakulev, V. A. Synthesis of novel thiazolidin-4-ones by reaction of malonthioamide derivatives with dimethyl acetylenedicarboxylate. *J. Chem. Soc., Perkin Trans. 1* **1998**, 2133−2136.
(32) Berseneva, V. S.; Morzherin, Y. Y.; Dehaen, W.; Luyten, I.; Bakulev, V. A. Reaction of heterocyclic thioamides with dimethyl acetylenedicarboxylate. Synthesis of novel 2-azolyl-5-methoxycarbonylmethylene thiazolin-4-ones. *Tetrahedron* **2001**, *57*, 2179−2184.
(33) Vallee, Y.; Chavant, P.-Y.; Pinet, S.; Pelloux-Leon, N.; Arnaud, R.; Barone, V. [4π + 2π] Cycloadditions of *N*-Acyl-Thioformamides. *Phosphorus, Sulfur Silicon Relat. Elem.* **1997**, *120*, 245.
(34) Baranac-Stojanović, M.; Tatar, M.; Stojanović, M.; Marković, R. Transformations of 2-alkylidene-4-oxothiazolidine vinyl bromides initiated by bromophilic attack of neutral and anionic nucleophiles. *Tetrahedron* **2010**, *66*, 6873−6884.
(35) Ho, Y. W.; Wang, I. J. Studies on the synthesis of some styryl-3-cyano-2(1*H*)-pyridinethiones and polyfunctionally substituted 3-aminothieno[2,3-*b*]-pyridine derivatives. *J. Heterocycl. Chem.* **1995**, *32*, 819−825.
(36) Frolov, K. A.; Dotsenko, V. V.; Krivokolysko, S. G. Mannich reaction in the synthesis of *N, S*-containing heterocycles. 15*. multicomponent cascade synthesis of 3,4,6a,7,8,9,10,10a-octahydro-2*H*,6*H*-pyrimido[4′,5′:4,5]pyrido[2,1-*b*][1,3,5]thia(Selena)-diazine derivatives. *Chem. Heterocycl. Compd.* **2013**, *48*, 1555−1561.
(37) Nesterov, V. N.; Antipin, M. Y.; Timofeeva, T. V.; Clark, R. D. Trans, trans-2-Cyano-5-(4-methoxyphenyl)penta-2,4-dienethioamide. *Acta Crystallogr., Sect. C: Cryst. Struct. Commun.* **2000**, *56*, 88−89.
(38) Nedolya, N. A; Brandsma, L.; Verkruijsse, H. D; van der Kerk, A. H.T.M; Trofimov, B. A Synthesis of derivatives of 2-imino-5,6-dihydro-2H-thiopyran from 1-heteroalkyl-1,3-butadienes and isothiocyanates. *Tetrahedron Lett.* **1998**, *39*, 2631−2634.
(39) Brandsma, L.; Schuijl, P. J. W. A convenient synthesis of 2*H*-thiopyran (Preliminary communication). *Rec. Trav. Chim.* **1969**, *88*, 30−32.
(40) Viehe, H. G.; Janousek, Z.; Merenyi, R.; Stella, L. The Captodative effect. *Acc. Chem. Res.* **1985**, *18*, 148−154.
(41) Sustmann, R.; Korth, H. G. The Captodative Effect. *Adv. Phys. Org. Chem.* **1990**, *26*, 131−178.
(42) Domingo, L. R.; Ríos-Gutiérrez, M.; Silvi, B.; Pérez, P. The mysticism of pericyclic reactions: a contemporary rationalisation of organic reactivity based on electron density analysis. *Eur. J. Org. Chem.* **2018**, *2018*, 1107−1120.
(43) Gómez-Pérez, J. R.; Delesma, F. A.; Calaminici, P.; Köster, A. M. Accuracy of auxiliary density functional theory hybrid calculations for activation and reaction enthalpies of pericyclic reactions. *J. Mol. Model.* **2018**, *24*, 223.
(44) López, C. S.; Faza, M.; Freindorf, O. N.; Kraka, E.; Cremer, D. Solving the Pericyclic-Pseudopericyclic Puzzle in the Ring-Closure Reactions of 1,2,4,6-Heptatetraene Derivatives. *J. Org. Chem.* **2016**, *81*, 404−414.
(45) Mouri, K.; Saito, S.; Hisaki, I.; Yamaguchi, S. Thermal 8π-electrocyclic reaction of heteroarene tetramers: new efficient access to π-extended cyclooctatetraenes. *Chem. Sci.* **2013**, *4*, 4465−4469.
(46) Calvo-Losada, S.; Quirante Sanchez, J. J. Pericyclic versus Pseudopericyclic Reactions. What the Laplacian of the Charge Density, $\nabla 2\rho(r)$, Has To Say about It? The Case of Cycloaddition Reactions. *J. Phys. Chem. A* **2008**, *112*, 8164−8178.
(47) Ayers, P. W.; Morell, C.; De Proft, F.; Geerlings, P. Understanding the Woodward-Hoffmann rules by using changes in electron density. *Chem. - Eur. J.* **2007**, *13*, 8240−8247.
(48) Bakulev, V. A. 1,6-Electrocyclic reactions. *Russ. Chem. Rev.* **1995**, *64*, 99−124.
(49) Bohórquez, H. J.; Matta, C. F.; Boyd, R. J. The localized electrons detector as an ab initio representation of molecular structures. *Int. J. Quantum Chem.* **2010**, *110*, 2418−2425.
(50) Johnson, E. R.; Keinan, S.; Mori-Sánchez, P.; Contreras-García, J.; Cohen, A. J.; Yang, W. Revealing noncovalent interactions. *J. Am. Chem. Soc.* **2010**, *132*, 6498−6506.
(51) Boto, R. A.; Contreras-García, J.; Tierny, J.; Piquemal, J. P. Interpretation of the reduced density gradient. *Mol. Phys.* **2016**, *114*, 1406−1414.
(52) Andrés, J.; Berski, S.; Contreras-García, J.; González-Navarrete, P. Following the Molecular Mechanism for the $NH_3 + LiH \rightarrow LiNH_2 + H_2$ Chemical Reaction: A Study Based on the Joint Use of the Quantum Theory of Atoms in Molecules (QTAIM) and Noncovalent Interaction (NCI) Index. *J. Phys. Chem. A* **2014**, *118*, 1663−1672.
(53) Valeur, B.; Berberan-Santos, M. N. *Molecular Fluorescence*, 2nd ed.; Wiley-VCH Verlag & Co.: Weinheim, Germany, 2013.
(54) Xiang, Z.; Wang, Z.-Y.; Ren, T.-B.; Xu, W.; Liu, Y.-P.; Zhang, X.-X.; Wu, P.; Yuan, L.; Zhang, X. B. A general strategy for development of a single benzene fluorophore with full-color-tunable, environmentally insensitive, and two-photon solid-state emission. *Chem. Commun.* **2019**, *55*, 11462−11465.
(55) Horvath, P.; Sebej, P.; Solomek, T.; Klan, P. Small-molecule fluorophores with large Stokes shifts: 9-iminopyronin analogues as clickable tags. *J. Org. Chem.* **2015**, *80*, 1299−1311.
(56) Li, J. Z.; Leng, T. H.; Wang, Z. Q.; Zhou, L.; Gong, X. Q.; Shen, Y. J.; Wang, C. U. A large Stokes shift, sequential, colorimetric fluorescent

https://dx.doi.org/10.1021/acs.joc.0c01934
J. Org. Chem. XXXX, XXX, XXX−XXX

probe for sensing Cu^{2+}/S^{2-} and its applications. *J. Photochem. Photobiol., A* **2019**, *373*, 146−153.
(57) Araneda, J. F.; Piers, W. E.; Heyne, D.; Parvez, M.; McDonald, R. High stokes shift anilido-pyridine boron difluoride dyes. *Angew. Chem., Int. Ed.* **2011**, *50*, 12214−12217.
(58) (b) Al-Otaibi, S. J.; Almuqrin, A. H.; Mary, Y. S.; Mary, Y. S. Comprehensive quantum mechanical studies on three bioactive anastrozole based triazole analogues and their SERS active graphene complex. *J. Mol. Struct.* **2020**, *1217*, 128388.
(59) Kim, K.-W.; Kwon, S.-H.; Lee, B.-J.; Ahn, S.-O.; Lee, J.-H.; Choi, J.-H. Synthesis and photophysical properties of fluorescent dyes based on triphenylamine, diphenylamine, diphenyl sulfone or triphenyltriazine derivatives containing an acetylene linkage group. *Dyes Pigm.* **2020**, *181*, 108617.
(60) Ozawa, T.; Yoshimura, H.; Kim, S. B. Advances in fluorescence and bioluminescence imaging. *Anal. Chem.* **2013**, *85*, 590−609.
(61) Carter, K. P.; Young, A. M.; Palmer, A. E. Fluorescent sensors for measuring metal ions in living systems. *Chem. Rev.* **2014**, *114*, 4564−4601.
(62) Eltyshev, A. K.; Minin, A. S.; Smoliuk, L. T.; Benassi, E.; Belskaya, N. P. 2-Aryl-2,4-dihydro-5*H*-[1,2,3]triazolo[4,5-*d*]pyrimidin-5-ones as a New Platform for the Design and Synthesis of Biosensors and Chemosensors. *Eur. J. Org. Chem.* **2020**, *2020*, 316−329.
(63) Schmidt, U.; Kubitzek, H. Synthesen mit den thioamiden der Malonsaure, Thiopyridone aus Cyan-thioacetamid. *Chem. Ber.* **1960**, *93*, 1559−1565.

https://dx.doi.org/10.1021/acs.joc.0c01934
J. Org. Chem. XXXX, XXX, XXX−XXX